Available online at www.sciencedirect.com
ScienceDirect
Phytochemistry 69 (2008) 894–910
PHYTOCHEMISTRY
www.elsevier.com/locate/phytochem

Phytoalexins and polar metabolites from the oilseeds canola and rapeseed: Differential metabolic responses to the biotroph *Albugo candida* and to abiotic stress

M. Soledade C. Pedras [a,*], Qing-An Zheng [a], Ravi S. Gadagi [a], S. Roger Rimmer [b]

[a] *Department of Chemistry, University of Saskatchewan, 110 Science Place, Saskatoon, SK, Canada S7N 5C9*
[b] *Saskatoon Research Centre, Agriculture and Agri Food Canada, 107 Science Place, Saskatoon, SK, Canada S7N 0X2*

Received 15 August 2007; received in revised form 1 October 2007
Available online 26 November 2007

Abstract

The metabolites produced in leaves of the oilseeds canola and rapeseed (*Brassica rapa* L.) inoculated with either different races of the biotroph *Albugo candida* or sprayed with $CuCl_2$ were determined. This investigation established consistent phytoalexin (spirobrassinin, cyclobrassinin, and rutalexin) and phytoanticipin (indolyl-3-acetonitrile, arvelexin, caulilexin C, and 4-methoxyglucobrassicin) production in canola and rapeseed in response to both biotic and abiotic elicitation. In addition, a wide number of polar metabolites were isolated from infected leaves, including six new phenylpropanoids and two new flavonoids. The extractable chemical components of zoosporangia of *A. candida* and the anti-oomycete activity of phytoalexins were determined as well. Overall, the results suggest that during the initial stage of the interaction, leaves of *B. rapa* have a similar response to virulent and avirulent races of *A. candida*, with respect to the accumulation of chemical defenses. After this stage, despite the higher phytoalexin concentration, the "compatible" races could overcome the plant defense system for further infection, but growth of the "incompatible" races was inhibited. Since results of bioassays showed that cyclobrassinin and brassilexin were more inhibitory to *A. candida* than rutalexin, the apparent redirection of the phytoalexin pathway towards rutalexin, avoiding cyclobrassinin and brassilexin accumulation might be caused by the pathogen. Alternatively, *A. candida* might be able to detoxify both cyclobrassinin and brassilexin, similar to necrotrophic plant pathogens. Overall, the correlation between phytoalexin production in infected or stressed leaves and the outcome of the plant–pathogen interaction suggested that *A. candida* was able to elude the plant defense mechanisms by, for example, redirecting the phytoalexin biosynthetic pathway.

Keywords: *Brassica rapa*; Rapeseed; Canola; Brassicaceae; Biotroph; Brassilexin; Cyclobrassinin; Defense response; Flavonoid; Indole glucosinolate; Oomycete; Rutalexin

1. Introduction

Canola (*Brassica rapa* subspecies *oleifera* L. or *B. napus* subspecies *oleifera* L.) is an oilseed crop of enormous economic significance in many countries of the world. The low content of saturated fatty acids of its oil has made it widely accepted by nutritionists and dieticians (Przybylski et al., 2005), while the protein content of the crushed seed made canola a very profitable crop. In addition to canola, the species *B. rapa* includes the oilseeds rapeseed/turnip rape, yellow and brown sarson, and the vegetables turnip, Chinese cabbage and pakchoi (Lim et al., 2006). Globally, these crops make a substantial contribution to the production of food, oil, and fodder. As with any major crops, stress posed by pests, diseases, salinity, and drought are a major constraint to sustainable agriculture production. For these reasons, it is of utmost importance to understand the general and specific responses of plants to biotic (e.g. fungi and bacteria) and abiotic (e.g. drought, metals) stress.

In general, the metabolic responses of plants vary according to the type of stress. These responses can be

* Corresponding author. Tel.: +1 306 966 4772; fax: +1 306 966 4730.
E-mail address: s.pedras@usask.ca (M.S.C. Pedras).

0031-9422/$ - see front matter © 2007 Elsevier Ltd. All rights reserved.
doi:10.1016/j.phytochem.2007.10.019

rather specific since the metabolic pool of plant defenses is composed of a variety of constitutive and induced metabolites. Phytoalexins are induced antimicrobial metabolites produced de novo by plants in response to biotic or abiotic stress, whereas phytoanticipins are constitutive metabolites with a defensive role (Pedras et al., 2007b). Although canola (*B. rapa*) was reported to produce several phytoalexins after $CuCl_2$ sprays (Rouxel et al., 1991), to date comprehensive defense metabolite profiles of the various *B. rapa* subspecies, including canola, do not appear to have been investigated. The metabolite profiles of phenylpropanoids in turnip leaves after insect infestation (Widarto et al., 2006) and methyl jasmonate sprays (Liang et al., 2006a, 2006b) were recently reported.

Obligate biotrophs are capable of penetrating and colonizing plant host tissues in ways that prevent immediate recognition by the host. It has been suggested that a biotroph may induce production or suppression of different proteins in the host, and suppress induced resistance mechanisms such as phytoalexin production and hypersensitive host cell death (Mendgen and Hahn, 2002; O'Connell and Panstruga, 2006). Recently, a mutant of *Arabidopsis thaliana* that accumulated significantly higher levels of the phytoalexin camalexin was reported to be more resistant than wild-type plants to virulent strains of the biotrophic pathogen *Hyaloperonospora parasitica* (Veronese et al., 2004). Nonetheless, little is known about the chemical defense pathways of plants, including phytoalexin elicitation and accumulation during biotrophic infections (Mendgen and Hahn, 2002; O'Connell and Panstruga, 2006).

The obligate biotrophic oomycete *Albugo candida* (Pers. ex Chev.) Kuntze causes white rust, an important disease of many cruciferous species, including canola (Pidskalny and Rimmer, 1985; Rolland et al., 2006). *A. candida* exhibits specialization on different cruciferous species and cultivars within a species (Rimmer et al., 2000). A number of races of *A. candida* have been classified based on specific pathogenicity to different *Brassica* species and cultivars. Isolates pathogenic to *B. rapa* were classified as race 7 and based on their virulence to the canola cultivar (cv.) Reward, these isolates were subgrouped as pathotype 7A (avirulent to cv. Reward, incompatible interaction) and pathotype 7V (virulent to rapeseed cv. Reward, compatible interaction). Other isolates were classified as race 2 based on their pathogenicity to brown mustard (*B. juncea* L.) and these were subgrouped as pathotype 2A (avirulent to cv. Cutlass, incompatible interaction) and pathotype 2V (virulent to cv. Cutlass, compatible interaction) (Rimmer et al., 2000). The interaction of races 2A and 2V with cvs. Torch and Reward are considered incompatible.

To understand the metabolic responses of canola and rapeseed to *A. candida*, we have investigated the kinetics of metabolite production and accumulation (polar and non-polar) in canola cvs. Torch (rapeseed) and Reward (canola) during infection. In addition, phytoalexin production in plants elicited by *A. candida* and abiotic elicitation using $CuCl_2$ were compared. Furthermore, we determined the anti-oomycete activity of these phytoalexins and the major chemical components of zoosporangia of *A. candida*. Overall, these studies demonstrate that canola and rapeseed (*B. rapa*) produce a metabolite blend similar in compatible interactions with *A. candida* but distinct of incompatible interactions and abiotic stress. Furthermore, the consistent phytoalexin blends produced in compatible interactions and their activity against *A. candida* appear to suggest that this pathogen can redirect the phytoalexin pathway to prevent production of more detrimental phytoalexins, e.g. rutalexin instead of cyclobrassinin and brassilexin.

2. Results

2.1. Phytoalexins and phytoanticipins from leaves of canola (*B. rapa*)

To determine the phytoalexins produced under biotic stress, the following interactions were investigated over a 10-day post-inoculation period: *B. rapa* cv. Torch ⟺ *A. candida* races 7V and 7A (compatible), and races 2V and 2A (incompatible) and *B. rapa* cv. Reward ⟺ *A. candida* races 7V(compatible), and races 7A, 2V and 2A (incompatible), as summarized in Fig. 1. In addition, to investigate the metabolites produced under abiotic stress, plants were sprayed with $CuCl_2$ and analyzed over a 10-day period.

Inoculation of leaves of *B. rapa* cvs. Torch and Reward with sporangia of *A. candida* (races 7V, 7A, 2V, and 2A) led to consistent elicitation of several phytoalexins. Five known phytoalexins, spirobrassinin (**1**), cyclobrassinin (**2**) rutalexin (**3**), rapalexin A (**4**), and rapalexin B (**5**) were detected in the non-polar extracts of leaves by HPLC analysis (Fig. 2 and Table 1). In addition, brassinin (**6**) was detected only in leaves of cv. Torch inoculated with race 7V. Within this group, rapalexins A (**4**) and B (**5**) are particularly interesting as they possess a unique aromatic isothiocyanate and were first isolated from canola/*B. rapa* (Pedras et al., 2007a). These metabolites were identified

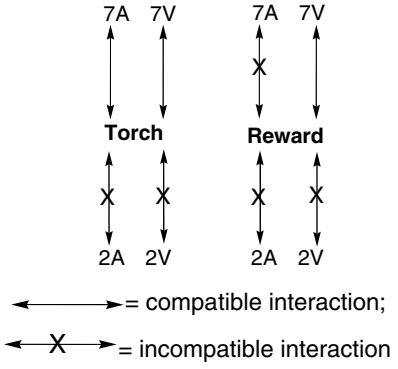

Fig. 1. Interaction of *Brassica rapa* cultivars Torch (rapeseed) and Reward (canola) with *Albugo candida* races 2A, 2V, 7A, and 7V.

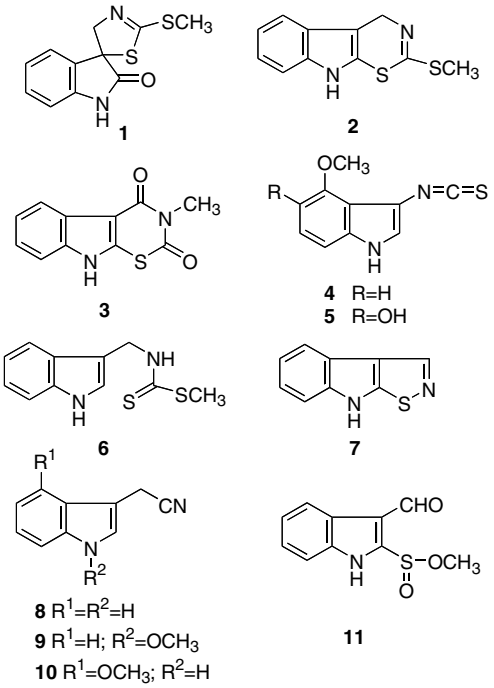

Fig. 2. Phytoalexins **1**–**7** and **11** and phytoanticipins **8**–**10** produced in leaves of *Brassica rapa* cultivars Torch (rapeseed) and Reward (canola) infected with *Albugo candida* races 2A, 2V, 7A, and 7V and sprayed with $CuCl_2$.

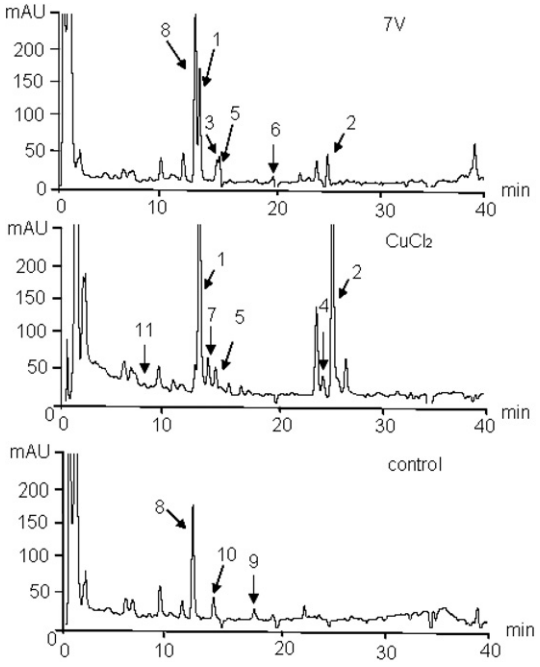

Fig. 3. HPLC chromatograms of non-polar extracts (using HPLC method A) of leaves of *Brassica rapa* cultivars Torch (rapeseed) and Reward (canola) elicited with *Albugo candida* race 7V, $CuCl_2$ and control leaves (numbers on peaks represent the compound numbers used in text and figures).

from their UV spectra, LC–MS data and comparison with authentic samples (Pedras et al., 2006).

Both biotic (*A. candida* races 2A, 2V, 7A, and 7V) and abiotic ($CuCl_2$) elicitation induced the production of spirobrassinin (**1**) and cyclobrassinin (**2**) in leaves of cvs. Torch and Reward, while rutalexin (**3**), rapalexins A (**4**) and B (**5**), brassinin (**6**), and brassilexin (**7**), were induced differentially (Table 1 and Fig. 3). In compatible interactions (Torch with 7A and 7V and Reward with 7V), spirobrassinin (**1**) was detected 2 days after biotic elicitation and had the highest concentration 7–8 days after inoculation (ca. 20–50 nmoles/g of fresh weight). In incompatible interactions (Torch with 2A and 2V and Reward with 2A, 2V, and 7A), spirobrassinin (**1**) was also detected 2 days after biotic elicitation but, contrary to the compatible interactions, showed the highest concentration much earlier (2–3 days after inoculation, ca. 7–10 nmoles/g of fresh weight). Upon elicitation with $CuCl_2$, the concentration of spirobrassinin (**1**) was ca. 4-fold higher than in compatible interactions, with the highest concentration found 2 days after spraying (ca. 167 nmol/g of fresh weight, Figs. 4 and 5). Similarly, cyclobrassinin (**2**) in compatible interactions (Torch with 7A and 7V and Reward with 7V) was detected 2 days after biotic elicitation and had the highest concentration 7–8 days after inoculation (ca. 15 nmoles/g of fresh weight). In incompatible interactions (Torch with 2A and 2V and

Table 1
Phytoalexins and phytoanticipins produced in leaves of *Brassica rapa* cultivars Torch (rapeseed) and Reward (canola) elicited with *Albugo candida* (races 2A, 2V, 7A, and 7V) and $CuCl_2$

Phytoalexins and phytoanticipins	*Brassica rapa*									
	cv. Torch (rapeseed)					cv. Reward (canola)				
	2A	2V	7A	7V	$CuCl_2$	2A	2V	7A	7V	$CuCl_2$
Spirobrassinin (**1**)	+	+	+	+	+	+	+	+	+	+
Cyclobrassinin (**2**)	+	+	+	+	+	+	+	+	+	+
Rutalexin (**3**)	+	+	+	+	–	+	+	+	+	–
Rapalexin A (**4**)	–	–	+	+	+	–	–	–	+	+
Rapalexin B (**5**)	–	–	+	+	+	–	–	+	+	+
Brassinin (**6**)	–	–	–	+	–	–	–	–	–	–
Brassilexin (**7**)	–	–	–	–	+	–	–	–	–	+
Indolyl-3-acetonitrile (**8**)	+	+	+	+	+	+	+	+	+	+
Caulilexin C (**9**)	+	+	+	+	+	+	+	+	+	+
Arvelexin (**10**)	+	+	+	+	+	+	+	+	+	+

Table 2
^{1}H NMR spectroscopic data (obtained in D_2O at 500 MHz) for compounds **14e–j** (δ in ppm, multiplicity, J in Hz)

Proton #	**14e**	**14f**	**14g**	**14h**	**14i**	**14j**
2′	7.06, *s*	6.81, *s*	7.23, *s*	6.83, *s*	7.13, *s*	6.89, *s*
3′	–	–	–	–	–	–
5′	7.11, *d*, 8	–	7.10, *d*, 8	–	7.03, *d*, 8	–
6′	6.94, *d*, 8	6.81, *s*	6.83, *d*, 8	6.83, *s*	6.79, *d*, 8	6.89, *s*
7′	7.69, *d*, 16	7.68, *d*, 16	7.68, *d*, 16	7.55, *d*, 16	7.54, *d*, 16	7.55, *d*, 16
8′	6.37, *d*, 16	6.39, *d*, 16	6.43, *d*, 16	6.34, *d*, 16	6.31, *d*, 16	6.34, *d*, 16
–OCH_3 (R^1/R^2)	3.76, *s*	3.95, *s*	3.78, *s*	3.74, *s*	3.75, *s*	3.75, *s*
2	5.64, *m*	5.65, *m*	5.52, *br s*	5.32, *m*	5.13, *d*, 5	5.13, *m*
3	3.00, *m*	3.00, *m*	2.88, *br s*	2.69, *m*	2.84, *br s*	2.85, *m*
–OCH_3 (R^3)	3.81, *s*	3.82, *s*	3.78	3.67, *s*	–	–
–OCH_3 (R^4)	3.76, *s*	3.76, *s*	–	–	3.61, s	3.60, *s*

Table 3
^{13}C NMR spectroscopic data (spectra obtained at 125 MHz) for compounds **14e–j** (δ in ppm)

Carbon #	**14e** ($CDCl_3$)	**14f** ($CDCl_3$)	**14g** (CD_3OD)	**14h** (D_2O)	**14i** (D_2O)	**14j** (D_2O)
1′	126.7	125.6	126.3	125.7	126.8	125.7
2′	108.1	105.1	110.3	106.3	111.5	106.5
3′	146.7	146.1	148.0	147.7	147.7	148.0
4′	148.2	137.2	149.4	136.0	148.0	137.5
5′	115.2	146.1	115.1	147.7	115.6	148.0
6′	123.6	105.1	122.5	106.3	123.4	106.5
7′	146.7	147.1	146.4	147.5	146.6	146.8
8′	113.8	113.2	113.2	113.2	114.1	113.2
9′	165.6	165.7	166.8	168.5	168.6	168.5
–OCH_3 (R^1/R^2)	55.9	56.3	55.1	56.3	56.9	56.3
1	169.5	169.5	170.6	177.1	175.8	177.1
2	67.9	68.1	69.5	70.7	71.6	70.7
3	35.9	36.0	37.2	38.9	36.7	38.9
4	169.5	169.5	170.6	172.7	173.2	173.2
–OCH_3 (R^3)	52.0	51.9	51.5	53.1	–	–
–OCH_3 (R^4)	52.5	52.6	–	–	52.6	52.5

Reward with 2A, 2V, and 7A), cyclobrassinin (**2**) was also detected 2 days after biotic elicitation but showed the highest concentration 2–3 days after inoculation (ca. 2–6 nmoles/g of fresh weight). However, the highest concentration of cyclobrassinin (**2**) was found 1–3 days after abiotic elicitation (20–30 nmol/g of fresh weight), as shown in Figs. 6 and 7. In the case of rutalexin (**3**), in compatible interactions (Torch with 7A and 7V and Reward with 7V), it was detected 3 days after biotic elicitation and showed the highest concentration 7–8 days after inoculation (ca. 16–30 nmoles/g of fresh weight). In incompatible interactions (Torch with 2A and 2V and Reward with 2A, 2V, and 7A), rutalexin (**3**) was also detected 3 days after biotic elicitation but, contrary to amounts in compatible interactions, it showed the highest concentration 3 days after inoculation (4–10 nmoles/g of fresh weight, Fig. 8). Interestingly, by contrast with spirobrassinin (**1**) and cyclobrassinin (**2**), rutalexin (**3**) was not detected in leaves of either Torch or Reward after elicitation with $CuCl_2$. Rapalexin B (**5**) was detected in leaves of cvs. Torch and Reward but only 5 days after inoculation with races 7A and 7V (1–8 nmoles/g of fresh weight). Abiotic elicitation induced production of rapalexin B (**5**) over the 10 days under study (2–6 nmoles/g of fresh weight), as shown in Figs. 9 and 10. Rapalexin A (**4**) was only detected 7 days after inoculation when Torch leaves were elicited with races 7A, 7V and Reward with race 7V (ca. 1 nmol/g of fresh weight, data not shown). When plants were elicited with $CuCl_2$, rapalexin A (**4**) was detected 1 day after elicitation with the highest concentration shown 2 days post-elicitation (1.5 nmoles/g of fresh weight). Brassinin (**6**) was detected only in cv. Torch inoculated with race 7V up to 5 days post-inoculation (highest concentration ca. 1.3 nmol/g of fresh weight, data not shown). Brassilexin (**7**) was only detected in leaves of Torch and Reward after abiotic elicitation and showed the highest concentration 3 days after inoculation (ca. 6 nmoles/g of fresh weight, Fig. 11). Similar to brassilexin (**7**), brassicanal C (**11**) was only detected in leaves of Torch and Reward after abiotic elicitation, but in very low amounts (data not shown). Furthermore, indolyl-3-acetonitrile (**8**), caulilexin C (**9**), and arvelexin (**10**) were detected in biotically and abiotically stressed leaves of cvs. Torch and Reward in higher amounts than in control plants (data not shown).

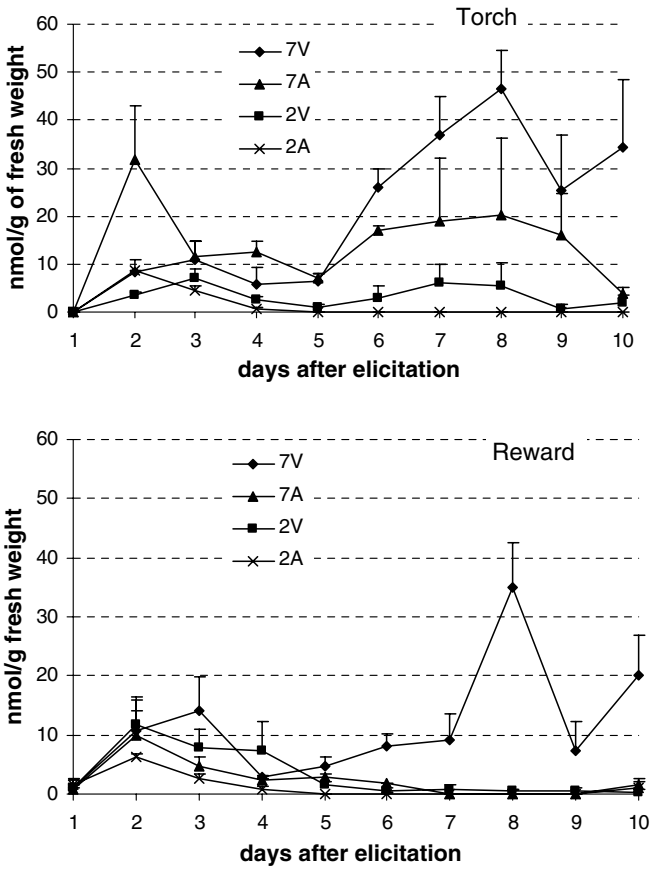

Fig. 4. Accumulation of spirobrassinin (**1**) in leaves of *Brassica rapa* cultivars Torch (rapeseed) and Reward (canola) inoculated with *Albugo candida* races 7V, 7A, 2V, 2A (bars represent standard deviations of at least nine independent determinations).

Fig. 5. Accumulation of spirobrassinin (**1**) in leaves of *Brassica rapa* cultivars Torch (rapeseed) and Reward (canola) sprayed with $CuCl_2$ (bars represent standard deviations of at least nine independent determinations).

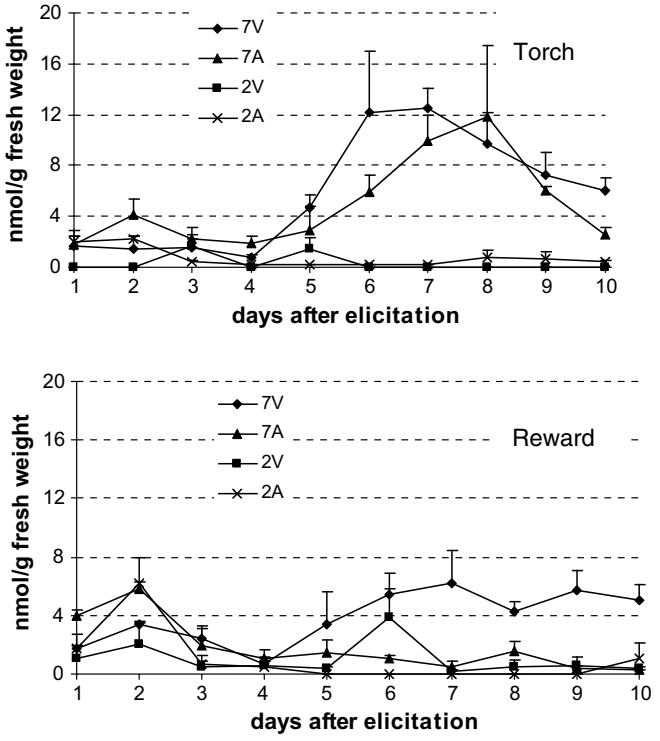

Fig. 6. Accumulation of cyclobrassinin (**2**) in leaves of *Brassica rapa* cultivars Torch (rapeseed) and Reward (canola) inoculated with *Albugo candida* races 7V, 7A, 2V, 2A (bars represent standard deviations of at least nine independent determinations).

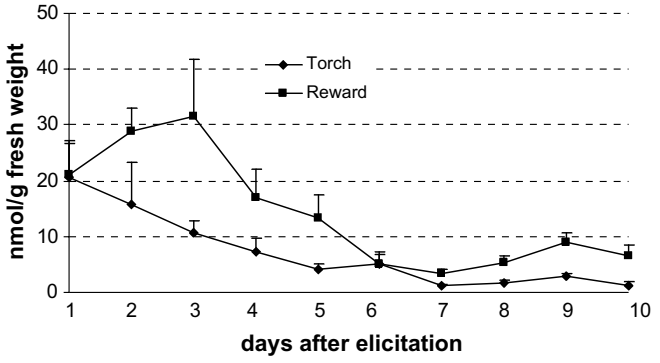

Fig. 7. Accumulation of cyclobrassinin (**2**) in leaves of *Brassica rapa* cultivars Torch (rapeseed) and Reward (canola) sprayed with $CuCl_2$ (bars represent standard deviations of at least nine independent determinations).

2.2. Polar metabolites from leaves of canola and rapeseed (*Brassica rapa*)

2.2.1. Isolation and identification of polar metabolites from leaves inoculated with *A. candida* 7V

The methanolic extract of leaves cv. Torch inoculated with *A. candida* race 7V (compatible interaction) was suspended in H_2O and extracted with CH_2Cl_2. The aqueous layer was fractionated first using Diaion HP-20 (H_2O–MeOH) followed by ODS-18, Sephadex LH-20 and silica gel to afford 44 compounds (**13a**–**25**), as described in Section 4. Of these metabolites, 36 were identified previously (Table in Supporting Data), and eight compounds (**14e**–**j**, **19g**, **19n**) are described here for the first time. Phenylpropanoids, including *p*-hydroxycinnamates of malic acid **14a**–**d** and its esters **14f**–**j** and glucosides **15a**–**d**, as well as flavonoids **19a**–**p** were the major components of the polar aqueous extracts. The structures of all metabolites were

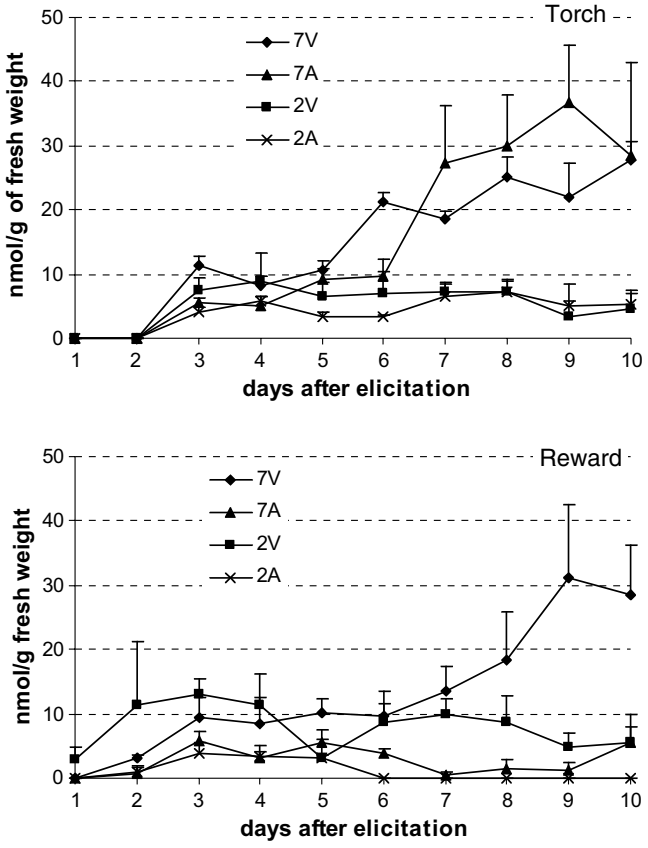

Fig. 8. Accumulation of rutalexin (**3**) in leaves of *Brassica rapa* cultivars Torch (rapeseed) and Reward (canola) inoculated with *Albugo candida* races 7V, 7A, 2V, 2A (bars represent standard deviations of at least nine independent determinations).

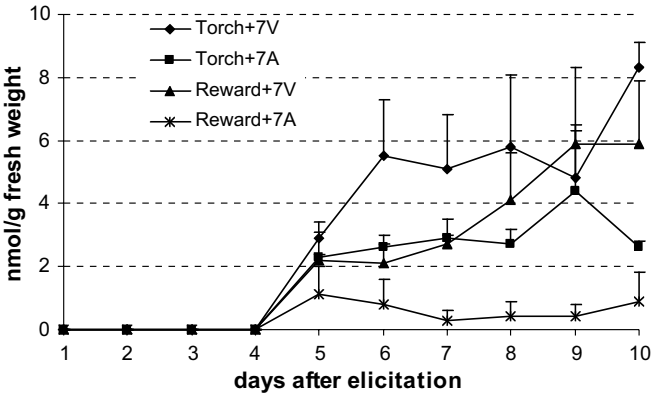

Fig. 9. Accumulation of rapalexin B (**5**) in leaves of canola (*Brassica rapa*) cultivars Torch and Reward inoculated with *Albugo candida* races 7V and 7A (bars represent standard deviations of at least nine independent determinations).

established by spectroscopic methods (namely NMR, HRMS, ESI-MS, UV), and in some cases chemical derivatization (methylation) or hydrolysis, and comparison with related or identical metabolites available in our crucifer metabolite library or comparison with reported data, as described below.

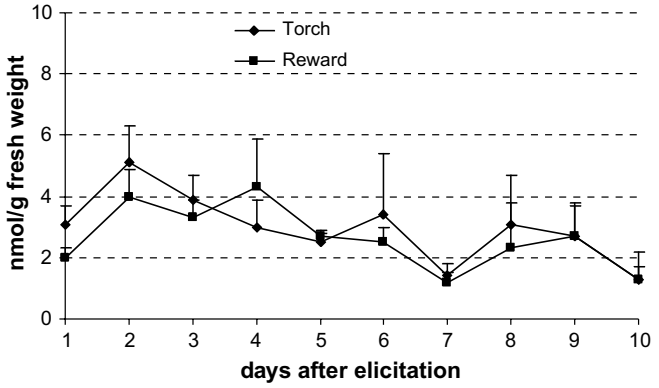

Fig. 10. Accumulation of rapalexin B (**5**) in leaves of *Brassica rapa* cultivars Torch (rapeseed) and Reward (canola) sprayed with $CuCl_2$ (bars represent standard deviations of at least nine independent determinations).

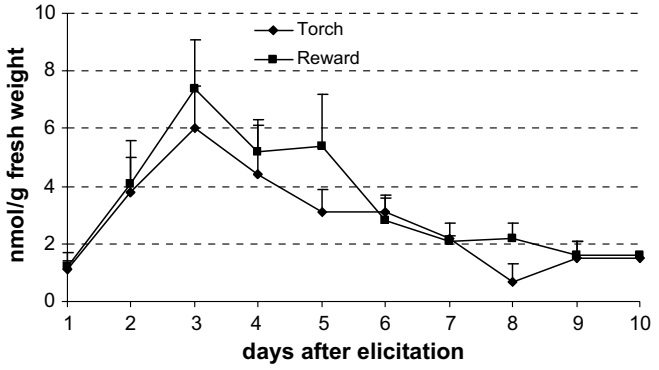

Fig. 11. Accumulation of brassilexin (**7**) in leaves of *Brassica rapa* cultivars Torch (rapeseed) and Reward (canola) sprayed with $CuCl_2$(bars represent standard deviations of at least nine independent determinations).

Indolyl glucosinolates **13a–c** were readily identified from their ESI-MS spectral data and ^{1}H NMR spectra, which established typical indolyl and methylene protons as well as all glucosyl protons (J of the anomeric H indicated β configuration, Fig. 12). The LC–MS data allowed immediate comparison with authentic samples available in our metabolite library.

The phenylpropanoids **14a–d** were identified as known hydroxycinnamates of malic acids based on NMR and ESI-MS spectroscopic data, and comparison with reported data (Liang et al., 2006a). The ^{1}H NMR spectra of **14a–j** showed the typical ABC spin system of 2-substituted malic acid in addition to aromatic and MeO protons of the phenyl group; the carbonyls were assigned from the ^{13}C NMR and HMBC spectroscopic data. The C–C double bond of the propenoyl moiety was assigned based on the typical *trans* coupling ($J = 16$ Hz) of α,β-propenoyl protons. In addition, malates **14e–j** were identified as the methyl esters of **14c** and **14d** (Fig. 13). The position of the methyl group was established from HMBC correlations. Compounds **14e–j** appear to be naturally occurring as they were present

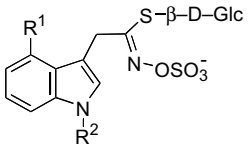

13a R^1 = H; R^2 = H
13b R^1 = OCH_3; R^2 = H
13c R^1 = H; R^2 = OCH_3

Fig. 12. Indole glucosinolates **13a–c** produced in leaves of *Brassica rapa* cultivars Torch (rapeseed) and Reward (canola) infected with *Albugo candida* races 2A, 2V, 7A, and 7V and sprayed with $CuCl_2$.

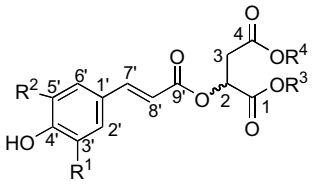

	R^1	R^2	R^3	R^4
14a	H	H	H	H
14b	OH	H	H	H
14c	OCH_3	H	H	H
14d	OCH_3	OCH_3	H	H
14e	OCH_3	H	CH_3	CH_3
14f	OCH_3	OCH_3	CH_3	CH_3
14g	OCH_3	H	CH_3	H
14h	OCH_3	OCH_3	CH_3	H
14i	OCH_3	H	H	CH_3
14j	OCH_3	OCH_3	H	CH_3

Fig. 13. Phenylpropanoid malates **14a–j** produced in leaves of *Brassica rapa* cultivars Torch (rapeseed) and Reward (canola) infected with *Albugo candida* races 2A, 2V, 7A, and 7V and sprayed with $CuCl_2$.

in plant extracts obtained with EtOAc or MeOH (these metabolites were not reported previously).

The phenylpropanoids **15a–d** were identified as known hydroxycinnamates of β-D-glucose based on NMR and ESI-MS spectroscopic data, and comparison with reported data (Harborne and Corner, 1961). The ^{1}H NMR spectra of **15a–c** showed the typical C–C double bond *trans* coupling ($J = 16$ Hz) of the propenoyl moiety whereas **15d** showed a *cis* coupling ($J = 12$ Hz), in addition to the aromatic and glucosyl protons (J of the anomeric H indicated β configuration). The structures of the glucosides **16** and **17** were assigned similarly, whereas **18** showed two distinct anomeric β-protons in addition to aromatic and tetrahydrofuranyl substituent. Finally, comparison with reported data (Thieme and Winkler, 1969; Gamal et al., 1997) allowed the assignment of the structures shown in Fig. 14.

Sixteen flavonol glycosides (**19a–p**) were isolated and characterized as having kaempferol (**19a–g**, **19o**, $R^1 = H$), quercetin (**19h–n**, $R^1 = OH$) and isorhamnetin (**19p**, $R^1 = OMe$) as aglycones, based on NMR and ESI-MS spectroscopic data. Isorhamnetin was present as isorhamnetin-3,7-di-*O*-β-D-glucopyranoside (**19p**) in higher quantities (>200 mg isolated from ca. 1 kg fresh leaves), while kaempferol and quercetin were present as glycosides or acylated glycosides (**19b–g**, **19i–n**, R^2 = acyl). The acyl groups were determined to be *p*-coumaroyl, caffeoyl, feruloyl, sinapoyl, and 5-hydroxyferuloyl. The aglycone of compounds **19a–f** and **19o** was identified as kaempferol (*p*-hydroxyphenyl) based on their ^{1}H NMR and ESI-MS spectroscopic data, which showed the typical 1,4-disubstitution in the phenyl ring (e.g. **19e**, δ_H 7.67, *d*, $J = 8.5$ Hz, 2H; 6.79, *d*, $J = 8.5$ Hz, 2H) (Nielsen et al., 1993). The C–C double bond of the acyl groups (R^2) attached to the outer glucosyl residue were assigned based on the typical *trans* coupling ($J = 16$ Hz) of α,β-acyl protons (Fig. 15). Furthermore, the structure of each acyl substituent (R^2) was established from the substitution pattern of the aromatic ring (NMR data) and ESI-MS. Positive ESI-MS data showed two typical signals for each acyl substituent (ion and acyl + glc ion; for coumaroyl, 147 and 309; caffeoyl, 163 and 325; feruloyl, 177, 339; sinapoyl, 207, 369; 5-hydroxyferuloyl, 193 and 355). The number of carbohydrate moieties was determined based on the number of anomeric protons observed in ^{1}H NMR spectra, which were well separated from other protons (δ_H 5–6 ppm). The larger coupling constants ($J = 7$–9 Hz) of the anomeric protons indicated the β configuration of the carbohydrate moieties. The linkages of the carbohydrate moieties were determined from HMBC data and/or by comparison with published data. The structures of these carbohydrates were assigned as glucosyl residues based on the chemical shifts observed in the ^{13}C NMR spectra and acid hydrolysis followed by comparison with D-glucose.

The aglycone of compounds **19h–m** was identified as quercetin (3′,4′-dihydroxyphenyl) based on their ^{1}H NMR signals and ESI-MS results. These flavonoids showed a typical ABX coupling system in the phenyl moiety of the aglycone (e.g., in **19j**. δ_H 7.33, s, 1H; 7.26, *d*,

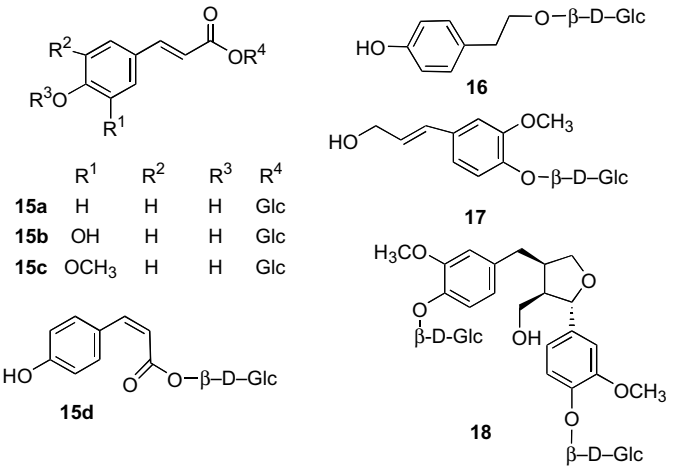

	R^1	R^2	R^3	R^4
15a	H	H	H	Glc
15b	OH	H	H	Glc
15c	OCH_3	H	H	Glc

15d

Fig. 14. Phenylpropanoids **15a–d**, **17** and **18** and phenylethanol glucoside **16** produced in leaves of *Brassica rapa* cultivars Torch (rapeseed) and Reward (canola) infected with *Albugo candida* races 2A, 2V, 7A, and 7V and sprayed with $CuCl_2$.

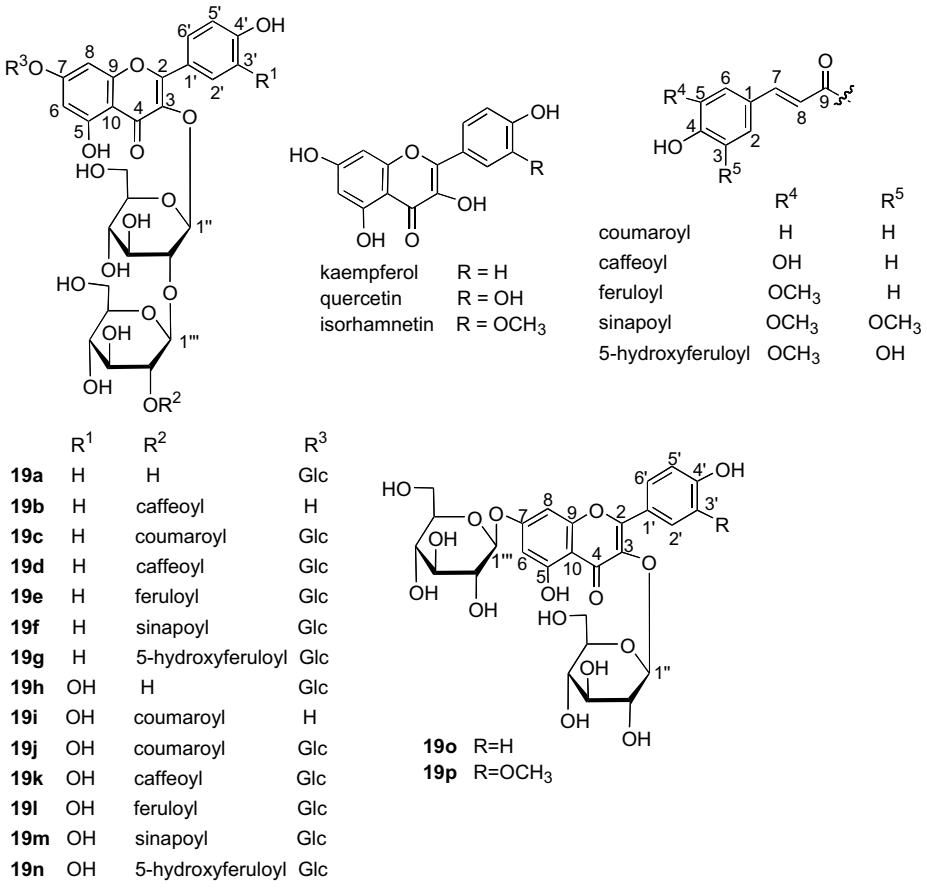

Fig. 15. Flavonoids **19a**–**p** produced in leaves of *Brassica rapa* cultivars Torch (rapeseed) and Reward (canola) infected with *Albugo candida* races 2A, 2V, 7A, and 7V and sprayed with $CuCl_2$.

$J = 8$ Hz, 1H; 6.78, *d*, $J = 8$ Hz, 1H) (Nielsen et al., 1993). As described above for flavonols **19a**–**g**, **19o**, the number of carbohydrate moieties was determined from the number of anomeric protons observed in the ^{1}H NMR spectra. As well, the structures of the acyl groups attached to the outer glucosyl residue were readily assigned based on the *trans* coupling of the α,β protons ($J = 16$ Hz) and the substitution pattern of aromatic rings.

Similarly, two new flavonoids, **19g** and **19n**, were isolated and their structures were established based on spectroscopic analysis. The aglycone of **19g** was established as kaempferol (4-hydroxyphenyl) based on the typical chemical shifts observed in the ^{1}H NMR spectrum (Table 4) as well as from ESI-MS data. The aglycone of **19n** was established as quercetin (3,4-dihydroxyphenyl) based on the typical chemical shifts observed in the ^{1}H NMR spectrum (Table 4) and ESI-MS data. Both **19g** and **19n** contained the acyl substituent 5-hydroxyferuloyl (R^2), which was deduced from the ESI-MS data (typical ions at *m/z* 193 and 355). In addition, their ^{1}H NMR spectra displayed two singlets (δ_H 5.99, 6.02) assignable to H-2 and H-6, and a *trans* C–C double bond. Furthermore, since both H-2 and H-6 showed a correlation with C-7 of the acyl group, the location of the MeO group was assigned as shown (Fig. 15). Both **19g** and **19n** contained three carbohydrate moieties (3 anomeric β-protons) deduced from the ^{1}H NMR spectroscopic data. NOESY spectral data indicated that one carbohydrate moiety was connected to C-7 of kaempferol since the anomeric proton (δ_H 5.02 ppm) of glucose displayed correlations to both C-6 and C-8 of kaempferol. The diglucosyl residue was deduced to be located at C-3 based on HMBC spectroscopic data and comparison with reported data (Nielsen et al., 1993). Furthermore, NOESY data showed a correlation of the anomeric proton of the inner carbohydrate moiety with the anomeric proton of the terminal carbohydrate moiety, which indicated the (1 → 2) bond between these carbohydrate moieties. A typical triplet (δ_H 4.83) belonging to H-2 of the terminal sugar moiety indicated that the acyl group was connected to C-2‴ which was also confirmed by HMBC data. Based on the above evidence, **19g** was deduced to be kaempferol-3-*O*-β-D-[2-*E*-5-hydroxyferuloyl-β-D-glucopyranosyl(1 → 2)-glucopyranoside]-7-*O*-β-glucopyranoside and **19n** was deduced to be quercetin-3-*O*-β-D-[2-*E*-5-hydroxyferuloyl-β-D-glucopyranosyl(1 → 2)-glucopyranoside]-7-*O*-β-glucopyranoside.

The NMR spectroscopic data of compound **19p** were similar to those of **19o**, but the typical 1,4-disubstitution in the phenyl ring of **19o** changed to an ABX system in **19p**, due to an extra methoxy group. This flavonoid

Table 4
NMR spectroscopic data (δ in ppm; δ_H at 500 MHz, J in Hz; δ_C at 125 MHz) for compounds **19g** and **19n** (in D_2O)

Carbon/ proton #	**19g**		**19n**	
	δ_H, multiplicity, J	δ_C	δ_H multiplicity, J	δ_C
2	–	156.4	–	156.4
3	–	133.2	–	133.7
4	–	177.3	–	177.7
5	–	159.3	–	159.8
6	6.24, *s*	99.2	6.18, *s*	99.7
7	–	161.9	–	162.4
8	6.21, *s*	94.7	6.09, *s*	95.1
9	–	155.3	–	155.8
10	–	106.0	–	106.5
1′	–	121.5	–	122.2
2′	7.78, *d*, 8	131.0	7.33, *s*	116.7
3′	6.88, *d*, 8	115.3	–	148.2
4′	–	158.8	–	144.1
5′	6.88, *d*, 8	115.3	6.84, *d*, 8	116.1
6′	7.78, *d*, 8	131.0	7.32, *d*, 8	123.1
1″	5.91, *d*, 7.5	95.9	5.90, *d*, 7.5	96.1
2″		79.7		80.2
3″		73.1		73.3
4″		69.4		69.6
5″		76.0[a]		76.4[b]
6″		60.1		60.4
1‴	5.20, *d*, 8	96.6	5.20, *d*, 8	96.9
2‴		73.1		73.6
3‴		73.9		74.1
4‴		69.3		69.8
5‴		75.9[a]		76.5
6‴		60.5		60.9
R^3 = Glc				
1⁗	5.02, *d*, 8	99.6	4.98, *d*, 8	100.1
2⁗		72.8		73.2
3⁗		75.4		75.8[b]
4⁗		69.4		69.8
5⁗		76.0[a]		76.5[b]
6⁗		60.6		60.9
R^2				
1	–	124.5	–	125.0
2	6.02, *s*	102.9	5.91, *s*	103.5
3	–	147.4	–	147.9
4	–	135.6	–	136.0
5	–	143.6	–	144.1
6	5.99, *s*	108.7	5.89, *s*	109.1
7	7.06, *d*, 16	145.7	6.95, *d*, 16	146.2
8	5.89, *d*, 16	113.4	5.89, *d*, 16	114.2
9	–	168.1	–	168.7
–OCH_3	3.42, *s*	55.3	3.37, *s*	55.8

[a,b] Assignment of carbons may be reversed.

structure matched with isorhamnetin. Therefore, **19p** was identified as isorhamnetin-3,7-di-*O*-β-D-glucopyranoside [**19p**], first isolated from *Argemone mexica* (Krishnamurti et al., 1965), and later found in many other species (e.g. Durkee and Harborne, 1973; Wolbis and Krolikowska, 1988).

Two ionone glycosides (**20a**, **20b**) were also isolated from polar extracts of leaves (Fig. 16). Their structures were established using 1D- and 2D NMR and ESI-MS spectroscopic data. From comparison with published data,

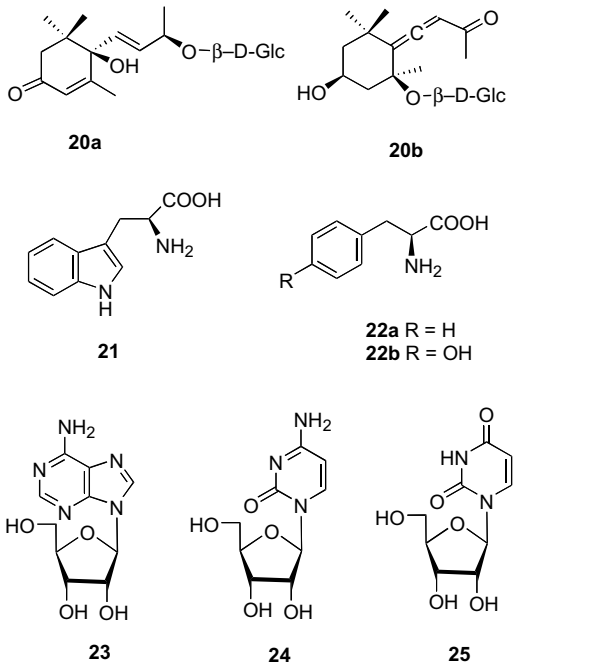

Fig. 16. Ionones **20a**, **20b**, amino acids **21**–**22b** and nucleotides **23**–**25** produced in leaves of *Brassica rapa* cultivars Torch (rapeseed) and Reward (canola) infected with *Albugo candida* races 2A, 2V, 7A , 7V and sprayed with $CuCl_2$.

the structures were assigned as roseoside (**20a**) and citroside A (**20b**) (Otsuka et al., 1995; Osorio et al., 1999). As well, L-tryptophan (**21**), L-phenylalanine (**22a**), L-tyrosine (**22b**), adenosine (**23**), cytidine (**24**), and uridine (**25**) were isolated from polar extracts, and their structures were established based on NMR data, ESI-MS analysis and comparison with authentic samples (Fig. 16).

Similarly, the polar metabolites described above were detected in cv. Reward as well. A table containing the name of each polar metabolite, the t_R (HPLC), and the pertinent references (reporting isolation and spectroscopic data) used here to confirm the structural assignments is provided in Supplementary data.

2.2.2. Quantification of polar metabolites

Polar metabolites of cvs. Torch and Reward elicited with *A. candida* races 7V, 7A, 2V, and 2A and $CuCl_2$ were extracted and analyzed over a 10-day post-elicitation period, as described in Section 4. Several types of polar metabolites, including indole glucosinolates, phenylpropanoids and phenylpropanoid glucosides, flavonoids and acyl glucosidic flavonoids, ionone glucosides, amino acids, and nucleotides were isolated and identified as described above. Quantitative analysis of metabolites available in sufficient amounts to construct calibration curves (HPLC-DAD) was carried out. Fig. 17 shows HPLC chromatograms of polar extracts of leaves elicited with *A. candida* and $CuCl_2$. The peaks corresponding to indole glucosinolates glucobrassicin (**13a**, $t_R = 4.4$ min), 4-methoxyglucobrassicin (**13b**, $t_R = 5.6$ min), 1-methoxyglucobrassicin (**13c**, $t_R =$

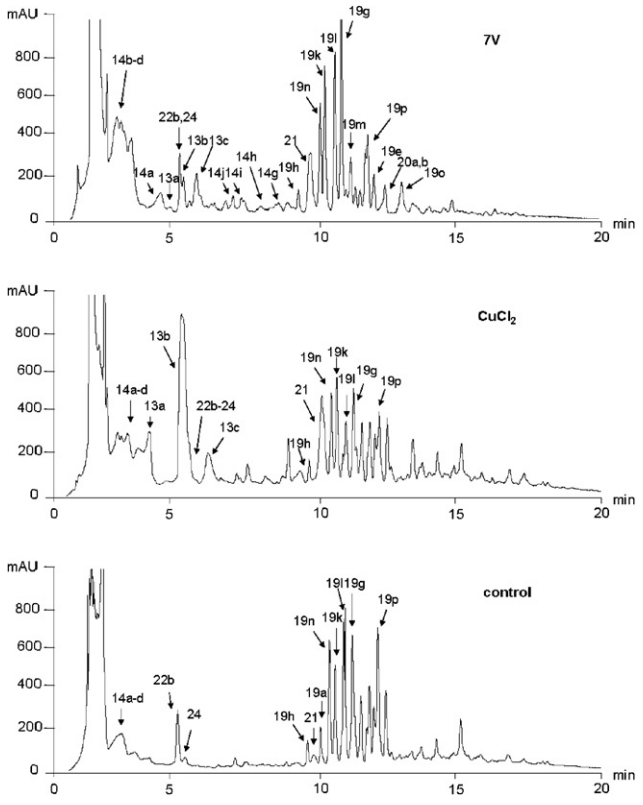

Fig. 17. HPLC chromatograms of polar extracts (using HPLC method B) of leaves of *Brassica rapa* cultivar Torch (rapeseed) elicited with *Albugo candida* race 7V, $CuCl_2$ and control leaves. (numbers on peaks represent the compound numbers used in text and figures).

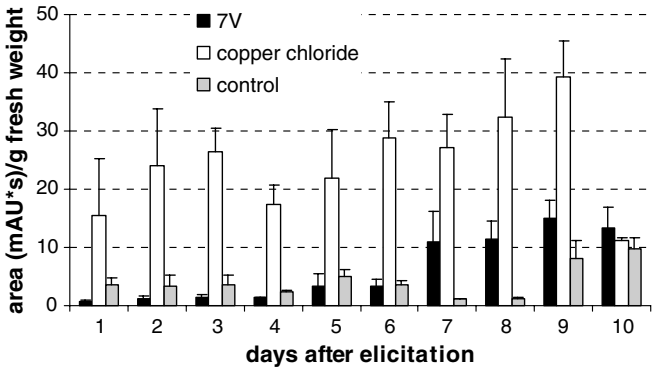

Fig. 18. Accumulation of 4-methoxyglucobrassicin (**13b**) in leaves of *Brassica rapa* cultivar Torch (rapeseed) inoculated with *Albugo candida* race 7V and sprayed with $CuCl_2$ (bars represent standard deviations of at least nine independent determinations).

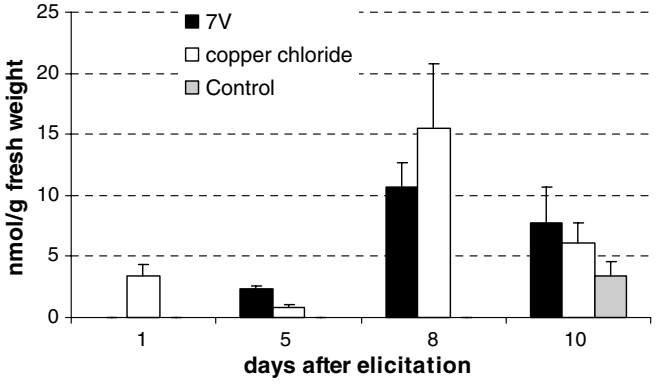

Fig. 19. Accumulation of tryptophan (**21**) in leaves of *Brassica rapa* cultivar Torch (rapeseed) inoculated with *Albugo candida* race 7V and sprayed with $CuCl_2$ (bars represent standard deviations of at least nine independent determinations).

6.5 min) and tryptophan (**21**, $t_R = 9.5$ min) indicated that these metabolites were present in larger amounts in extracts of leaves sprayed with $CuCl_2$ than in controls or inoculated leaves. However, quantification of these compounds was not quite accurate because this region is rather congested and thus a few peaks overlapped. For example, glucobrassicin (**13a**, $t_R = 4.4$ min) overlapped with **14a**, 4-methoxyglucobrassicin (**13b**, $t_R = 5.6$ min) overlapped with tyrosine (**22b**) and cytidine (**24**), 1-methoxyglucobrassicin (**13c**, $t_R = 6.5$ min) overlapped with **14j**, and tryptophan (**21**, $t_R = 9.5$ min) overlapped with **19a**. Despite the overlapping peaks, it was clear that 4-methoxyglucobrassicin (**13b**, Fig. 18, due to peak overlap, relative amounts are shown in mAU) and tryptophan (**21**, Fig. 19) concentrations changed significantly in sprayed and infected leaves. The highest concentrations of 4-methoxyglucobrassicin (**13b**) and tryptophan (**21**) were detected in leaves of cv. Torch sprayed with $CuCl_2$ 8 days after elicitation; elicitation with *A. candida* 7V had a similar but less noticeable effect. However, when plant leaves were elicited with races 2V or 2A, 4-methoxyglucobrassicin (**13b**), and tryptophan (**21**) concentrations were similar to control leaves.

The flavonoids containing kaempferol (**19a**) and quercetin (**19h**, **19k**, and **19n**) were quantified in leaves collected 1, 5, 8, and 10 days after elicitation. In most of the samples, there were no significant differences compared with the corresponding control samples. Samples infected with *A. candida* showed slightly lower concentrations at later stages compared to control samples, while samples sprayed with $CuCl_2$ produced similar or higher amounts than control samples (Figs. S1–S4 in Supplementary Data).

2.3. Metabolites from zoosporangia of *A. candida*

Chemical analysis (HPLC-DAD, HPLC-MSD, and NMR) of a dichloromethane extract of zoosporangia of *A. candida* races 2V and 7V showed that the main components of the extracts were triacylglycerols of C_{18} fatty acids (ca. 25 mg per g of zoosporangia), the phytoalexins spirobrassinin (**1**, 7 nmoles.g^{-1} of zoosporangia) and rapalexins A (**4**) and B (**5**) ($\leqslant$2 nmoles g^{-1} of zoosporangia). The aqueous extract contained the non-reducing disaccharide trehalose (α-D-glucopyranosyl-1,1-α-D-glucopyranoside) as the major component (37 mg g^{-1} of zoosporangia). The chemical structure of trehalose was established by comparison of its high-resolution mass spectrometric data and ^1H and ^{13}C NMR spectroscopic data with those of an authentic

sample of trehalose commercially available and published data (Bock et al., 1983).

2.4. Anti-oomycete activity of metabolites

Two bioassays were developed to evaluate the activity of phytoalexins and other compounds against *A. candida* races 2V and 7V: (i) zoosporangia viability measured by zoospore release from sporangia (Mitani et al., 2001) and (ii) germination of encysted zoospores, hereon called cysts, on a cellulose membrane (Francis et al., 1996; Von Röpenack et al., 1998). Thirteen compounds, including the phytoalexins spirobrassinin (**1**), cyclobrassinin (**2**), rutalexin (**3**), rapalexins A (**4**) and B (**5**), brassinin (**6**), brassilexin (**7**), and brassicanal C (**11**), the fungicide thiabendazole (5, 10 and 50 μM) and two fungicide mixtures (benomyl and ridomil, 5, 10 and 50 mg l^{-1}) were tested at three concentrations (Tables 5 and 6). After incubation of zoosporangia in aqueous solutions containing the test compounds, zoospores were counted and the percentage of inhibition on zoospore release was calculated relative to controls (Table 5). Cyclobrassinin (**2**) and brassilexin (**7**) inhibited completely the release of zoospores of *A. candida* races 2V and 7V at 10 μM, whereas brassinin (**6**) showed a similar effect at 50 μM. Spirobrassinin (**1**), rutalexin (**3**), indolyl-3-acetonitrile (**8**), and caulilexin C (**9**) inhibited ca. 60–90% the release of zoospores of both races at 50 μM. Indole-3-carboxaldehyde (**12**) had no effect on the zoospore release of both races even at the highest concentration (50 μM). The fungicides benomyl and ridomil MZ showed a stronger effect (complete inhibition at 50 mg l^{-1}) than thiabendazole (slight effect at 50 μM).

Table 5
Inhibition[a] of zoospore release from zoosporangia of *Albugo candida* races 2V and 7V

Compounds	*A. candida* race 2V			*A. candida* race 7V		
	5 μM	10 μM	50 μM	5 μM	10 μM	50 μM
Spirobrassinin (**1**)	3 ± 1	68 ± 2	81 ± 5	29 ± 1	62 ± 8	91 ± 9
Cyclobrassinin (**2**)	95 ± 5	100 ± 0	100 ± 0	94 ± 6	100 ± 0	100 ± 0
Rutalexin (**3**)	17 ± 3	40 ± 6	77 ± 9	32 ± 3	43 ± 9	57 ± 4
Rapalexin A (**4**)	100 ± 0	100 ± 0	100 ± 0	100 ± 0	100 ± 0	100 ± 0
Rapalexin B (**5**)	0	42 ± 2	91 ± 4	1 ± 0	33 ± 5	78 ± 5
Brassinin (**6**)	53 ± 8	73 ± 4	100 ± 0	52 ± 11	100 ± 0	100 ± 0
Brassilexin (**7**)	95 ± 4	100 ± 0	100 ± 0	97 ± 3	100 ± 0	100 ± 0
Indolyl-3-acetonitrile (**8**)	80 ± 12	92 ± 8	94 ± 2	38 ± 1	78 ± 4	84 ± 1
Caulilexin C (**9**)	54 ± 5	62 ± 3	82 ± 7	62 ± 1	73 ± 1	85 ± 0
Indole-3-carboxaldehyde (**12**)	0	0	0	0	0	0
Thiabendazole (fungicide)	0	0	16 ± 9	0	0	0
Fungicide mixture	5 mg/l	10 mg/l	50 mg/l	5 mg/l	10 mg/l	50 mg/l
Benomyl	54 ± 3	73 ± 8	100 ± 0	57 ± 11	75 ± 11	100 ± 0
Ridomil MZ	82 ± 5	93 ± 2	100 ± 0	70 ± 11	90 ± 3	100 ± 0

[a] Percentage of inhibition calculated as reported in the experimental (each value represents the mean and standard deviation of at least nine independent determinations).

Table 6
Inhibition[a] of cyst germination of *Albugo candida* races 2V and 7V

Compounds	*A. candida* race 2V			*A. candida* race 7V		
	5 μM	10 μM	50 μM	5 μM	10 μM	50 μM
Spirobrassinin (**1**)	13 ± 3	56 ± 5	76 ± 1	0	61 ± 3	94 ± 3
Cyclobrassinin (**2**)	65 (± 11)	84 (± 15)	100 (± 2)	72 (± 7)	97 (± 1)	100 (± 0)
Rutalexin (**3**)	0	16 ± 14	57 ± 13	18 ± 3	41 ± 6	59 ± 12
Rapalexin A (**4**)	15 ± 3	71 ± 2	100 ± 0	18 ± 4	75 ± 4	100 ± 0
Rapalexin B (**5**)	5 ± 3	46 ± 16	100 ± 0	10 ± 5	35 ± 6	74 ± 6
Brassinin (**6**)	7 (± 3)	91 (± 3)	100 (± 0)	11 (± 4)	73 (± 3)	100 (± 0)
Brassilexin (**7**)	43 (± 15)	100 (± 5)	100 (± 6)	56 (± 2)	96 (± 4)	100 (± 0)
Indolyl-3-acetonitrile (**8**)	25 (± 5)	52 (± 4)	79 (± 7)	25 (± 5)	52 (± 4)	79 (± 7)
Caulilexin C (**9**)	0	0	13 (± 5)	0	16 (± 6)	29 (± 3)
Indole-3-carboxaldehyde (**12**)	0	0	0	0	0	0
Thiabendazole (fungicide)	0	5 ± 1	7 ± 2	0	0	7 ± 2
Fungicide mixture	5 mg/l	10 mg/l	50 mg/l	5 mg/l	10 mg/l	50 mg/l
Benomyl	42 ± 6	83 ± 6	100 ± 0	55 ± 1	85 ± 6	100 ± 0
Ridomil MZ	0	50 ± 1	100 ± 0	0	54 ± 4	100 ± 0

[a] Percentage of inhibition calculated as reported in the experimental (each value represents the mean and standard deviation of at least nine independent determinations).

Germination of cysts of *A. candida* races 2V and 7V on cellulose dialysis membranes immersed in different concentrations of test solutions and inoculated with motile zoospores of *A. candida* races 2V and 7V were incubated and the number of germinated cysts were counted. Phytoalexins and test compounds showed a similar inhibitory effect on cyst germination of *A. candida* races 2V and 7V as on zoospore release (Table 6). For example, brassilexin and cyclobrassinin inhibited completely cyst germination of *A. candida* races 2V and 7V at 10 μM and brassinin inhibited completely the cyst germination at 50 μM. Furthermore, thiabendazole was not toxic to *A. candida* 2V and 7V even at 50 μM, whereas ridomil MZ inhibited ca. 50% of cyst germination at 10 mg/l and benomyl inhibited ca. 83% of cyst germination at 10 mg/l.

3. Discussion and conclusion

3.1. Phytoalexins, phytoanticipins, and polar metabolites from leaves of canola and rapeseed (*B. rapa*)

The interaction of *B. rapa* cvs. Torch and Reward with four races of *A. candida* provided a model to analyze metabolic responses in compatible and incompatible interactions between a crucifer and a biotroph (Fig. 1). This work established for the first time consistent phytoalexin production in response to inoculation with a biotroph (*A. candida* races 2V, 2A, 7V, and 7A). To the best of our knowledge, this is the first time that differential phytoalexin production in response to elicitation by a biotrophic oomycete is demonstrated. Interestingly, the accumulation of spirobrassinin (**1**), cyclobrassinin (**2**), and rutalexin (**3**) in leaves inoculated with races 7V, 7A, 2A, or 2V was similar during the first 4 days. Afterwards, the concentrations of these three phytoalexins became lower and eventually undetectable in incompatible interactions, while in compatible interactions the concentrations of these phytoalexins became higher, with the highest concentration at 7–10-days post-inoculation. These results suggest that during the initial stage of the interaction, leaves of *B. rapa* have a similar response to avirulent and virulent races of *A. candida* with respect to the accumulation of chemical defenses. After this stage, despite the higher phytoalexin concentration, the "compatible" races could overcome the plant defense system for further infection, but growth of the "incompatible" races was inhibited. These results are consistent with previous findings (Chou et al., 2000) reporting that the induction of invertase activity and defense proteins occurred very rapidly in leaves of *A. thaliana* after the initial challenge with *A. candida* in the incompatible interaction. By contrast, in compatible interactions (*A. candida–A. thaliana*) invertase activity, accumulation of sugars, and the repression of photosynthetic gene expression occurred several days after infection.

The different amounts of cyclobrassinin (**2**), rutalexin (**3**), and brassilexin (**7**) produced in infected plants and in $CuCl_2$ sprayed plants (Figs. 6–8 and 11, lower amounts of cyclobrassinin (**2**) and higher amounts of rutalexin (**3**) in infected leaves but no rutalexin in sprayed leaves) suggest that these metabolites (and/or their biosynthetic precursors) play an important role in the plant–pathogen interaction. Since results of bioassays (Tables 5 and 6) showed that cyclobrassinin (**2**) and brassilexin (**7**) were stronger inhibitors of *A. candida* than rutalexin (**3**), an apparent redirection of the phytoalexin pathway towards rutalexin (**3**) avoiding cyclobrassinin (**2**) and brassilexin (**7**) accumulation might be caused by the pathogen. This exchange would favor the pathogen and would be consistent with the lack of brassilexin (**7**) production in infected plants (brassilexin (**7**) is produced only in $CuCl_2$ sprayed leaves). This hypothesis appears reasonable since cyclobrassinin (**2**) is a biosynthetic precursor of both rutalexin (**3**) and brassilexin (**7**) and the biosynthesis of rutalexin from cyclobrassinin is unlikely to involve more than three enzymatic steps (oxidation, hydrolysis, and methylation) (Pedras et al., 2007b). Alternatively, *A. candida* might be able to detoxify both cyclobrassinin (**2**) and brassilexin (**7**), similar to necrotrophic fungi (Pedras and Ahiahonu, 2005). Although indolyl-3-acetonitrile (**8**), arvelexin (**10**), and caulilexin C (**9**) were previously reported as phytoalexins of a few plant species (Pedras et al., 2007b), these metabolites are phytoanticipins but not phytoalexins in cv. Torch and Reward because they were detected in control leaves and their production increased upon elicitation. Previously, in a study using 43 accessions of *Brassica* species, it was found that a *B. rapa* line 29 produced the phytoalexins cyclobrassinin (**2**), brassilexin (**7**), and cyclobrassinin sulfoxide 48 h after spraying with $CuCl_2$ (Rouxel et al., 1991).

Different types of polar metabolites, including esters and glucosides of hydroxycinnamic acid and their malic derivatives, flavonoids, ionone glucosides, amino acids, and nucleotides were isolated from leaves of cv. Torch infected with *A. candida*. Among this large pool, quantitative differences were detected in leaf extracts by HPLC for indole glucosinolates and tryptophan (**21**, Fig. 19). In fact the production of 4-methoxyglucobrassicin (**13b**) was substantially higher in sprayed leaves than in control leaves. This result is consistent with the accumulation of higher amounts of arvelexin (**10**, $t_R = 14.5$ min) in sprayed leaves, as glucosinolates are known to give nitriles, isothiocyanates, etc., upon enzymatic degradation (Bones and Rossiter, 2006). As well, since crucifer phytoalexins are biosynthesized from tryptophan (**21**), an increase of its concentration was expected; the highest concentration of tryptophan was detected 8 days after elicitation. Nonetheless, since tryptophan is a biosynthetic precursor of many different metabolites, its concentration increase could be related with other biosynthetic pathways. Previously, it was reported that polar metabolites from cruciferous plants, including glucosinolates (Fahey et al., 2001), polar indole metabolites (Hahlbrock et al., 2003), soluble compounds (Hagemeier et al., 2001), and wall-bound phenolics (Tan et al., 2004)

were induced and might play important roles in crucifer defense. Glucosyl indole-3-carboxylic acids were identified from *A. thaliana* roots infected with *Pythium sylvaticum* (Bednarek et al., 2005). As well, monolignol glucosides, e.g. coniferin (**17**), were characterized from *A. thaliana* roots infected with *P. sylvaticum* but their biological functions were not established (Whetten and Sederoff, 1995).

Naturally occurring phenylpropanoids such as hydroxycinnamic acid, caffeic acid, ferulic acid, and sinapic acid can be present in plants as glucose esters and glucosides, or as esters of organic acids, such as quinic acid, malic acid, and tartaric acid. The six new methyl malates **14e–j** were isolated from canola leaves and their structures were established using spectroscopic data and comparison with the corresponding free acid derivatives. To the best of our knowledge these metabolites have not been reported to date. Previously, the four hydroxycinnamoyl malic acids **14a–d** as well as 5-hydroxyferuloyl malic acid were detected and characterized in extracts of turnip leaves by NMR analysis (Liang et al., 2006a, 2006b). As well, the hydroxycinnamoyl malic acids **14a–d** were isolated from radish (Brandl et al., 1984). These phenolic derivatives appeared to be related with UV resistance but not with pathogen defense (Li et al., 1993; Hagemeier et al., 2001). In our work, no substantial quantitative differences in the accumulation of these metabolites were detected in biotically or abiotically stressed canola leaves.

Overall, the correlations observed between phytoalexin production in infected leaves of canola and rapeseed (biotrophic elicitation) and the outcome of the plant-pathogen interaction suggest that *A. candida* is able to elude the plant defense mechanisms by, for example, redirecting the phytoalexin biosynthetic pathway. Considering that none of the genes involved in the brassica phytoalexin pathway are known currently, it is unlikely that this hypothesis can be confirmed soon. Notwithstanding this outlook, additional analysis of canola cultivars resistant and susceptible to *A. candida* could provide stronger evidence for the significance of the phytoalexin pathway. In addition, considering both the non-polar and polar metabolite profiles, it is clear that canola metabolic responses to the biotroph *A. candida* are distinct from responses to abiotic stress.

3.2. Anti-oomycete activity of phytoalexins and metabolites from zoosporangia of A. candida

The main chemical components of zoosporangia of *A. candida* races 2V and 7V were determined to ensure that induced metabolites (detected or isolated) were produced by canola leaves and not by sporangia. We determined that zoosporangia contained the phytoalexin spirobrassinin (**1**, 7 nmoles/g of zoosporangia), rapalexins A (**4**) and B (**5**, <2 nmoles/g of zoosporangia) and trehalose (37 mg/g of zoosporangia). To the best of our knowledge, no similar data have been published previously. The presence of spirobrassinin (**1**) was not surprising since this is a phytoalexin produced in leaves of many brassicas including brown mustard (*B. juncea*), canola and rapeseed (*B. rapa*) from where zoosporangia of races 2V and 7V were isolated (spirobrassinin may adhere to zoosporangia surface). On the other hand, rapalexins A (**4**) and B (**5**) are much less abundant than spirobrassinin (**1**) and thus their presence was less expected. Nonetheless, because these compounds are induced by $CuCl_2$ as well, there is no doubt that they are produced by the plant. Trehalose is a storage carbohydrate in microorganisms accumulated mainly during starvation conditions and has been connected with stress protection (Rolland et al., 2006), as well as thermo- and cryo-protector and protein stabilizer (Voit, 2003). Trehalose is one of the most important storage carbohydrates as it is present in almost all living organisms except mammals (Benaroudj et al., 2001).

It is worthy to note that the phytoalexins cyclobrassinin (**2**), rapalexin A (**4**), and brassilexin (**7**) displayed substantially more potent inhibitory activity against zoospore release at much lower concentrations (ca. 2 mg/l) than the commercial fungicides benomyl and ridomil MZ (ca. 50 mg/l). Because ridomil MZ was found to be one of the most active fungicides for treatment of *A. candida* infections (Godika and Pathak, 2005), our results suggest that rapalexin A (**4**) could be a good lead structure to develop natural protection agents. It would be of great interest to analyze lines of *Brassica* species to determine if the production of cyclobrassinin (**2**), rapalexin A (**4**), and brassilexin (**7**) correlates positively with resistance to *A. candida*.

4. Experimental

4.1. General

All chemicals were purchased from Sigma–Aldrich Canada Ltd., Oakville, Ont. All solvents were analytical grade except for high performance liquid chromatography (HPLC) grade solvents used for HPLC analysis. HPLC analysis was carried out with an HPLC system equipped with quaternary pump, automatic injector and diode array detector (DAD, wavelength range 190–600 nm), degasser and a Hypersil ODS column (5 μm particle size silica, 200 × 6 internal diameter mm) equipped with an in-line filter. HPLC method A: linear gradient of H_2O–CH_3CN (75:25) to H_2O–CH_3CN (0:100) for 35 min, with flow rate 1.0 ml/min; method B: isocratic H_2O–CH_3CN (80:20) for 10 min, linear gradient of H_2O–CH_3CN (80:20) to H_2O–CH_3CN (40:60) for 10 min, H_2O–CH_3CN (40:60) to H_2O–CH_3CN (25:75) for 10 min, with a flow rate 1.0 ml/min. Liquid chromatography–mass spectrometry (LC–MS) data were obtained using an Agilent 1100 series HPLC system (Agilent Technologies, USA) equipped with an autosampler, binary pump, degasser, a DAD connected directly to a mass detector (MSD, Agilent G2440A MSD-Trap-XCT ion trap mass spectrometer) with an

electrospray ionization (ESI) source. Chromatographic separation was carried out at room temperature using an Eclipse XSB C-18 column (5 μm particle size silica, 150 mm × 4.6 mm internal diameter). The mobile phase consisted of a gradient of 0.2% HCO_2H in H_2O (A) and 0.2% HCOOH in CH_3CN (B) (75% A to 75% B in 35 min, to 100% B in 5 min) and a flow rate of 1.0 ml/min. Additional conditions for the MSD were as previously reported (Pedras et al., 2006).

Crucifer phytoalexins were synthesized as previously reported (Pedras et al., 2007b) with purities above 98% (determined by HPLC-DAD and ^1H NMR spectroscopy). Calibration curves were prepared for each phytoalexin using synthetic samples dissolved in CH_3CN to prepare stock solutions, followed by serial dilutions. Calibration curves were prepared using peak areas of the HPLC chromatograms obtained using method A or B, as necessary (A for non-polar compounds, B for more polar compounds). The correlation coefficients of phytoalexin calibration curves were $\geqslant 0.9998$.

NMR spectra were recorded on 500 MHz spectrometers. For ^1H NMR spectra (500 MHz) the chemical shifts (δ) are reported in parts per million (ppm) relative to TMS. The δ values were referenced to $CDCl_3$ ($CHCl_3$ at 7.28 ppm), CD_3CN (CD_2HCN at 1.94 ppm), CD_3OD (CD_2HOD at 4.87 ppm), D_2O (HDO at 4.79 ppm). For ^{13}C NMR spectra (125.8 MHz) the chemical shifts (δ) were referenced to $CDCl_3$ (77.4 ppm), CD_3OD (49.0 ppm). The multiplicities of the ^{13}C signals refer to the number of attached protons: $s = C$, $d = CH$, $t = CH_2$, $q = CH_3$. Fourier transform infrared (FT-IR) data were recorded on a spectrometer and spectra were measured by the diffuse reflectance method on samples dispersed in KBr. Ultraviolet (UV) spectra were recorded on a spectrophotometer using a 1 cm path length quartz cell.

4.2. Plant material and isolates of *A. candida*

B. rapa cvs. Torch (rapeseed) and Reward (canola) were sown in individual pots in peat-lite at day/night temperature 20/16 °C, and 16 h photoperiod (250 μmol s^{-1} m^{-2}). Seven-day-old or fully expanded cotyledons and 14-day-old leaves were used for inoculation. For time course analysis by HPLC, three individual plants in separate pots were used as replicates for each cultivar, with three leaves per plant collected and extracted as reported below.

A. candida races 2V, 2A and 7V and 7A used in this study were obtained from Agriculture and Agri-Food Canada, Saskatoon Research Centre. The isolates were multiplied by inoculation on cotyledons and/or leaves of brown mustard (*B. juncea*) cv. Commercial Brown (races 2V and 2A) and canola (*B. rapa*) cv. Torch (races 7V and 7A) as reported by Liu et al. (1996).

4.3. Inoculum preparation and quantification

The inoculum was prepared as previously reported (Liu et al., 1996). In brief, zoosporangia (10 mg) were added to sterile distilled H_2O (50 ml in a 100 ml Erlenmeyer flask), the flask was swirled to suspended zoosporangia followed by incubation at 16 °C for 3 h (no shaking). The emerging motile zoospore suspension was kept on ice to maintain zoospore motility. The number of zoospores was counted under a light microscope (40×) using a haemocytometer. Prior to placing the cover glass on the spore haemocytometer, a Q-tip soaked in formalin was held near the drop of zoospores for a few seconds, to stop zoospores from moving before counting was initiated. The zoospore suspension was adjusted to 10^6 spores/ml.

4.4. Biotic and abiotic elicitation of canola and rapeseed (*B. rapa* cultivars Torch and Reward) and preparation of extracts for time-course analysis

A. candida races 2A, 2V, 7A and 7V were used for biotic elicitation. Two-week-old leaves of cvs. Torch and Reward were inoculated with zoospore suspensions of (10 μl droplets of zoospore inocula on leaf surfaces, 6–8 droplets per leaf) and plants were incubated in a growth chamber in the dark for 24 h at 16 °C, at 100% relative humidity. After 24 h, the chamber environment was changed to the growth conditions described above. Abiotic elicitation was carried out spraying plants with $CuCl_2$ (1×10^{-3} M). After elicitation, the plants were incubated in a growth chamber under conditions described above. Samples (three leaves per plant) were collected every 24 h after elicitation up to 10 days. Leaves (500–800 mg) were frozen and ground in liquid N_2 and extracted with MeOH (6–8 ml) on a shaker at 120 rpm for 3 h. The leaf solids were removed by filtering and the solvent was evaporated to give a concentrated sample. The resulting oily residue was rinsed with CH_2Cl_2 (5 ml) and the remaining solid residue (polar extract) dissolved in MeOH–H_2O (1:1, 200 μl) for HPLC analysis. The CH_2Cl_2 extract (non-polar fraction) was concentrated under reduced pressure and dissolved in CH_3CN (60 μl) for HPLC analysis.

4.5. Isolation and identification of polar metabolites from leaves of rapeseed (*B. rapa*) cv. Torch

After incubation for 7 days in a growth chamber, infected leaves (1.3 kg) of cv. Torch were collected, frozen in liquid N_2, ground, and extracted with MeOH (2×6 l). The solvent was concentrated under reduced pressure (1 l) and the suspension was partitioned with CH_2Cl_2 (2×1 l). The aqueous phase was passed through a Diaion HP-20 column (200 g), eluted with H_2O–MeOH to obtain fraction 1 (7.5 g, H_2O) and fraction 2 (7.5 g, MeOH), respectively. Fraction 1 was further purified using ODS-18 (eluted with H_2O–MeOH) and Sephadex LH-20 (eluted with H_2O–MeOH) to yield **22b** (5 mg), **24** (4 mg), **25** (2 mg), **23** (45 mg), **14e** (3 mg), **14f** (7 mg), **14g** (5 mg), **14h** (15 mg), **14i** (2 mg) and **14j** (7 mg). Fraction 2 (7.5 g) was subjected to ODS-18 chromatography using H_2O–MeOH (100:0–30:70) to yield six fractions: 2A (1.3 g, H_2O), 2B (0.9 g, H_2O–MeOH, 95:5), 2C

(1.5 g, H_2O–MeOH, 90:10), 2D (1.6 g, H_2O–MeOH, 80:20), 2E (1.2 g, H_2O–MeOH, 70:30), 2F (0.8 g, H_2O–MeOH, 60:40). Fraction 2A was further purified using ODS-18 (eluted with H_2O–MeOH) and Sephadex LH-20 (eluted with H_2O–MeOH) to yield: **13a** (5 mg), **13b** (4 mg), **13c** (2 mg), **14a** (7 mg), **14b** (45 mg), **14c** (12 mg) and **14d** (6 mg). Fraction 2B was further purified by repeated chromatography on ODS-18, Sephadex LH-20 and silica gel to yield: **19a** (16 mg), **19h** (10 mg), **19g** (38 mg), **19k** (22 mg), **19n** (26 mg) and **21** (14 mg). Fraction 3B was further purified by repeated chromatography on ODS-18, Sephadex LH-20 and silica gel to yield: **18** (2 mg), **16** (5 mg), **17** (3 mg), **19c** (17 mg), **19d** (23 mg), **19j** (17 mg), **19l** (37 mg), **19m** (4 mg), **19e** (5 mg), **19f** (6 mg) and **22a** (15 mg). Fraction 4B was further purified by repeated chromatography on ODS-18, Sephadex LH-20 and silica gel to yield: **15a** (5 mg), **15b** (3 mg), **15c** (3 mg), **15d** (4 mg), **19b** (17 mg), **19i** (15 mg), **19o** (12 mg), **19p** (230 mg), **20a** (15 mg) and **20b** (12 mg).

4.5.1. Characterization of new metabolites

Dimethyl feruloyl malate (**14e**). HPLC, $t_R = 24.1$ min. ESI-MS (negative, *m/z*, relative abundance): 337.3 (100), 193.9 (5). ESI-MS (positive, *m/z*, relative abundance): 361.4 (50), 339.2 (20), 177.3 (100), 143.6 (40), 117.6 (15). HR-ESI-MS (negative): *m/z* 337.0926, 337.0928 calc. for $C_{16}H_{17}O_8$ [M^+-1]. For ^{1}H NMR (500.2 MHz in $CDCl_3$) and ^{13}C NMR (125.8 MHz in $CDCl_3$): see Tables 2 and 3. λ_{max} (MeOH)/nm: 220 (log ε, 4.10), 236 (log ε, 4.09), 328 (log ε, 4.29).

Dimethyl sinapoyl malate (**14f**). HPLC, $t_R = 24.3$ min. ESI-MS (negative, *m/z*, relative abundance): 367.5 (100). ESI-MS (positive, *m/z*, relative abundance): 391.4 (34), 369.3 (10), 207.3 (100), 175.4 (30), 147.5 (10), 119.5 (9). HR-ESI-MS (negative): *m/z* 367.1026, 367.1034 calc. for $C_{17}H_{19}O_9$ [M^+-1]. For ^{1}H NMR (500.2 MHz in $CDCl_3$) and ^{13}C NMR (125.8 MHz in $CDCl_3$) spectra, see Tables 2 and 3. λ_{max} (MeOH)/nm: 204 (log ε, 4.36), 239 (log ε, 4.29), 331 (log ε, 4.36).

Methyl feruloyl malate (**14g**). HPLC, $t_R = 8.4$ min. ESI-MS (negative, *m/z*, relative abundance): 323.2 (100), 292.1 (65), 195.0 (20). ESI-MS (positive, *m/z*, relative abundance): 347.2 (50), 325.2 (6), 177.2 (100), 145.3 (85), 117.5 (15). HR-ESI-MS (negative): *m/z* 323.0770, 323.0772 calc. for $C_{15}H_{15}O_8$ [M^+-1]. For ^{1}H NMR (500.2 MHz in CD_3OD): ^{13}C NMR (125.8 MHz in CD_3OD): see Table 3. λ_{max} (MeOH)/nm: 236 (log ε, 4.04), 328 (log ε, 4.23).

Methyl sinapoyl malate (**14h**). HPLC, $t_R = 8.8$ min. ESI-MS (negative, *m/z*, relative abundance): 353.2 (100), 322.4 (50). ESI-MS (positive, *m/z*, relative abundance): 377.2 (20), 355.1 (15), 207.2 (100), 175.4 (70), 147.5 (15), 119.5 (10). HR-ESI-MS (negative): *m/z* 353.0872, 353.0878 calc. for $C_{16}H_{17}O_9$ [M^+-1]. For ^{1}H NMR (500.2 MHz in D_2O): and ^{13}C NMR (125.8 MHz in D_2O): spectroscopic data, see Tables 2 and 3 λ_{max} (MeOH)/nm: 241 (log ε, 4.09), 328 (log ε, 4.09).

Methyl feruloyl malate (**14i**). HPLC, $t_R = 7.9$ min. ESI-MS (negative, *m/z*, relative abundance): 323.1 (40), 193.2 (100), 130.0 (4). ESI-MS (positive, *m/z*, relative abundance): 347.2 (30), 307.2 (6), 177.2 (100), 145.2 (90), 117.4 (15). HR-ESI-MS (negative): *m/z* 323.0766, 323.0772 calc. for $C_{15}H_{15}O_8$ [M^+-1]. For ^{1}H NMR (500.2 MHz in D_2O) and ^{13}C NMR (125.8 MHz in D_2O) spectroscopic data, see Tables 2 and 3. λmax (MeOH)/nm: 235 (log ε, 4.01), 324 (log ε, 4.19).

Methyl sinapoyl malate (**14j**). HPLC, $t_R = 7.8$ min. ESI-MS (negative, *m/z*, relative abundance): 353.2 (80), 223.4 (100). ESI-MS (positive, *m/z*, relative abundance): 377.2 (20), 337.2 (17), 207.2 (100), 175.3 (70), 147.5 20), 119.6 (15). HR-ESI-MS (negative): *m/z* 353.0914, 353.0878 calc. for $C_{16}H_{17}O_9$ [M^+-1]. For ^{1}H NMR (500.2 MHz in D_2O) and ^{13}C NMR (125.8 MHz in D_2O) spectroscopic data, See Tables 2 and 3. λ_{max} (MeOH)/nm: 247 (log ε, 4.09), 328 (log ε, 4.09).

Kaempferol-3-*O*-β-D-[2-*E*-5-hydroxyferuloyl-β-D-glucopyranosyl(1 → 2)-glucopyranoside]-7-*O*-β-D-glucopyranoside (**19g**). HPLC, $t_R = 10.8$ min. ESI-MS (negative, *m/z*, relative abundance): 963.7 (100). ESI-MS (positive, *m/z*, relative abundance): 965.3 (20), 803.3 (M^++1−Glc) (10), 611.4 (M^++1−Glc-5-hydroxyferuloyl) (80), 449.4 (75), 355.4 (100), 193.3 (25). HR-ESI-MS (negative): *m/z* 963.2349, 963.2411 calc. for $C_{43}H_{47}O_{25}$ [M^+-1]. For ^{1}H NMR (500.2 MHz in D_2O) and ^{13}C NMR (125.8 MHz in D_2O): spectroscopic data, See Tables 4. λ_{max} (MeOH)/nm: 209 (log ε, 4.28), 244 (log ε, 4.48), 268 (log ε, 4.47), 333 (log ε, 4.43).

Quercetin 3-*O*-β-D-[2-*E*-5-hydroxyferuloyl-β-D-glucopyranosyl(1 → 2)glucopyranoside]-7-*O*-β-D-glucopyranoside (**19n**). HPLC, $t_R = 10.3$ min. ESI-MS (negative, *m/z*, relative abundance): 979.7 (100). ESI-MS/MS (negative, *m/z*, relative abundance): 981.3 (30), 817.8 (100), 788.9 (25), 626.1 (26). HR-ESI-MS (negative): *m/z* 979.2340, 979.2361 calc. for $C_{43}H_{47}O_{26}$ [M^+-1]. For ^{1}H-NMR (500.2 MHz in D_2O) and ^{13}C NMR (125.8 MHz in D_2O) spectroscopic data, see Table 4. λ_{max} (MeOH)/nm: 206 (log ε, 4.56), 224 (log ε, 4.49), 249 (log ε, 4.53), 340 (log ε, 4.45).

4.6. Acid hydrolysis of glucosides

A solution of compounds **19g** and **19n** (2 mg each) in 5% HCl (0.5 ml) was heated (90 C) for 2 h. After concentration to dryness, the mixture was diluted with H_2O (3 ml) and filtered through a micropipette containing ODS-18 (0.5 g) and eluted with H_2O (5 ml). The aqueous solution was concentrated and analyzed by TLC ($CHCl_3$–MeOH–H_2O, 7:3:0.5) to compare with carbohydrate standards.

4.7. Anti-oomycete activity

4.7.1. Inhibition of zoospore release from sporangia

Sporangia of *A. candida* 2V and 7V (ca. 10 mg) were added to a 250 ml Erlenmeyer flask containing 100 ml of 10% MeOH in sterile distilled H_2O (v/v) and the flask

was swirled to suspend zoosporangia. This zoosporangium suspension (10 ml) was dispensed into 20 ml vials and then 10 μl of the test solution (phytoalexin or compound in DMSO) was added to vials to make final concentrations of 5, 10, and 50 μM, respectively. Stock solutions of fungicides benomyl and ridomil MZ were made in 10% aqueous MeOH, and then were added to assay vials to make final concentrations of 5, 10, and 50 μg/ml. DMSO (10 μl) was added to control assay vials. All vials were incubated for at 16 °C, in complete darkness for 3 h. The experiments were repeated three times with six replications. Mobile zoospores were counted using a haemocytometer under a phase contrast microscope (40×) and the percentage inhibition relative to controls was calculated according to the following equation: % inhibition = [(# zoospores in control solution − # zoospores in test solution)/# zoospores in control solution] × 100.

4.7.2. Inhibition of cyst germination on cellulose dialysis membrane

A cellulose dialysis membrane (Cuprophan, Medicell International Ltd., London, UK) was cut into ca. 1 cm squares and autoclaved. The autoclaved dialysis membrane pieces were placed on 2% H_2O agar to ensure even hydration (Francis et al., 1996). After 24 h, the membrane pieces were dipped separately in solutions of phytoalexins or fungicides at the concentrations 5, 10, and 50 μM of phytoalexin and 5, 10, and 50 μg/ml of fungicide in 10% aqueous MeOH and each piece placed back on agar; solutions were allowed to evaporate in laminar flow hood for 15 min. For controls, cellulose dialysis membranes were dipped in 10% aqueous MeOH and solutions were allowed to evaporate in laminar flow hood for 15 min. A suspension of zoospores of *A. candida* (10 μl) was added to each membrane piece and plates were incubated at 16 C, in complete darkness for 24 h. Cyst germination was assessed under a phase contrast microscope (40×) and the percentage of inhibition of cyst germination was calculated according to the following equation: % inhibition = [(# cyst germinated in control solution − # cyst germinated in test solution)/# cyst germinated in control solution] × 100.

4.8. Extraction of zoosporangia of A. candida

Zoosporangia of *A. candida* races 2V and 7V were obtained from leaves of 21-day-old *B. juncea* cv. Commercial Brown and *B. rapa* cv. Torch, respectively, as previously reported (Rimmer et al., 2000). Zoosporangia (300 mg) were suspended in EtOAc (2 ml) and then sonicated; after 20 min, the solvent was separated from zoosporangia by filtration and concentrated under reduced pressure using a rotary evaporator. The extracted zoosporangia were resuspended in MeOH (2 ml) and sonicated for further 20 min. The MeOH extract was separated by filtration and concentrated; zoosporangia were autoclaved and discarded. Both organic extract residues were combined (19 mg), concentrated and the residue was rinsed with dichloromethane (2 ml) to yield a dichloromethane extract (7.6 mg) and a residue that was soluble in MeOH (7 mg) or H_2O (4.8 mg). Each extract was subjected to HPLC-DAD, HPLC-MSD, and NMR analysis to determine the chemical components.

Acknowledgments

Support for the authors' work was obtained from the Natural Sciences and Engineering Research Council of Canada (Accelerator Grants for Exceptional New Opportunities to M.S.C.P.), Canada Foundation for Innovation, Canada Research Chairs Program (M.S.C.P.), and the University of Saskatchewan.

Appendix A. Supplementary data

Supplementary data associated with this article can be found, in the online version, at doi:10.1016/j.phytochem.2007.10.019.

References

Bednarek, P., Schneider, B., Svatos, A., Oldham, N.J., Hahlbrock, K., 2005. Structural complexity, differential response to infection, and tissue specificity of indolic and phenylpropanoid secondary metabolism in Arabidopsis roots. Plant Physiology 138, 1508–1570.

Benaroudj, N., Lee, D.H., Goldberg, A.L., 2001. Trehalose accumulation during cellular stress protects cells and cellular proteins from damage by oxygen radicals. Journal of Biological Chemistry 276, 24261–24267.

Bock, K., Defaye, J., Driguez, H., Bar-Guilloux, E., 1983. Conformation in solution of α, α-trehalose, α-D-glucopyranosyl, α-D-mannopyranose and their 1-thioglycosyl analogs and a tentative correlation of their behavior with respect to the enzyme trehalose. European Journal of Biochemistry 131, 595–600.

Bones, A.M., Rossiter, J.T., 2006. The enzymic and chemically induced decomposition of glucosinolates. Phytochemistry 67, 1053–1067.

Brandl, W., Herrmann, K., Grotjahn, L.Z., 1984. Hydroxycinnamoyl esters of malic acid in small radish (*Raphanus sativus* Lvar. *sativus*). Zeitschrift fur Naturforschung 39c, 515–520.

Chou, H.M., Bundock, N., Rolfe, S.A., Scholes, J.D., 2000. Infection of *Arabidopsis thaliana* leaves with *Albugo candida* (white blister rust) causes a reprogramming of host metabolism. Molecular Plant Pathology 1, 99–113.

Durkee, A.B., Harborne, J.B., 1973. Flavonol glycosides in *Brassica* and *Sinapis*. Phytochemistry 12, 1085–1089.

Fahey, J.W., Zalcmann, A.T., Talalay, P., 2001. The chemical diversity and distribution of glucosinolates and isothiocyanates among plants. Phytochemistry 56, 5–51.

Francis, S.A., Dewey, F.M., Gurr, S.J., 1996. The role of cutinase in germling development and infection by *Erysiphe graminis* fsp. *hordei*. Physiological and Molecular Plant Pathology 49, 201–211.

Gamal, A.A.El., Takeya, K., Itokawa, H., Halim, A.F., Amer, M.M., Saad, H.E.A., 1997. Lignan bis-glucosides from *Galum sinaicum*. Phytochemistry 45, 597–600.

Godika, S., Pathak, A.K., 2005. Control of white rust and Alternaria blight diseases of mustard by foliar sprays of Ridomil. Pestology 29, 9–10.

Hagemeier, J., Schneider, B., Oldham, N., Hahlbrock, K., 2001. Accumulation of soluble and wall-wound indolic metabolites in *Arabidopsis thaliana* leaves infected with virulent or avirulent *Pseudomonas*

syringae pathovar tomato strains. Proceedings of the National Academy of Science of the USA 98, 753–758.

Hahlbrock, K., Bednarek, P., Ciokowski, I., Hamberger, B., Heise, A., Liedgens, H., Logemann, E., Nurnberger, T., Schmelzer, E., Somssich, I.E., Tan, J., 2003. Non-self recognition, transcriptional reprogramming, and secondary metabolite accumulation during plant/pathogen interaction. Proceedings of the National Academy of Science of the USA 100, 14569–14576.

Harborne, J.B., Corner, J.J., 1961. Plant polyphenols 4hydroxycinnamic acid–sugar derivatives. Biochemical Journal 81, 242.

Krishnamurti, M., Ramanathan, J.D., Seshadri, T.R., Sharkaran, P.R., 1965. Flavonol glycosides of *Argemone mexicane* flowers. Indian Journal of Chemistry 3, 270–272.

Li, J.Y., Ou-Lee, T.M., Rabas, R., Amundson, R.G., Last, R.L., 1993. Arabidopsis flavonoid mutants are hypersensitive to UV-B irradiation. Plant Cell 5, 171–179.

Liang, Y.S., Choi, Y.H., Kim, H.K., Linthorst, H.J.M., Verpoorte, R., 2006a. Metabolomic analysis of methyl jasmonate treated *Brassica rapa* leaves by 2-dimensional NMR spectroscopy. Phytochemistry 67, 2503–2511.

Liang, Y.S., Kim, H.K., Lefeber, A.W.M., Erkelens, C., Choi, Y.H., Linthorst, H.J.M., Verpoorte, R., 2006b. Identification of phenylpropanoids in methyl jasmonate treated Brassica rapa leaves using two-dimensional nuclear magnetic resonance spectroscopy. Journal of Chromatography A 1112, 148–155.

Lim, Y.P., Prikshit, P., Su, R.C., Taesik, U., Chang, P.H., Jae, W.B., Yoon, K.H., 2006. Toward unraveling the structure of *Brassica rapa* genome. Physiologia Plantarum 126, 585–591.

Liu, J.Q., Parks, P., Rimmer, S.R., 1996. Development of monogenic lines for resistance to *Albugo candida* from a Canadian *Brassica napus* cultivar. Phytopathology 86, 1000–1004.

Mendgen, K., Hahn, M., 2002. Plant infection and the establishment of fungal biotrophy. Trends in Plant Science 7, 352–356.

Mitani, S., Araki, S., Yamaguchi, T., Takii, Y., Ohshima, T., Matsuo, N., 2001. Antifungal activity of the novel fungicide cyazofamid against *Phytophthora infestans* and other plant pathogenic fungi *in vitro*. Pesticide Biochemistry and Physiology 70, 92–99.

Nielsen, J.K., Olsen, C.E., Petersen, M.K., 1993. Acylated flavonol glycosides from cabbage leaves. Phytochemistry 34, 539–544.

O'Connell, R.J., Panstruga, R., 2006. Tete a tete inside a plant cell: establishing compatibility between plants and biotrophic fungi and oomycetes. New Phytologist 171, 699–718.

Osorio, C., Duque, C., Fujimoto, Y., 1999. C13-Norisoprenoid glucoconjugates from Lulo (*Solanum quitoense* L) leaves. Journal of Agriculture and Food Chemistry 47, 1641–1645.

Otsuka, H., Yao, M., Kamada, K., Takeda, Y., 1995. Alangionosides G-M: Glycosides of Megastigmane derivatives from the leaves of *Alangium premnifolium*. Chemical and Pharmaceutical Bulletin 43, 754–759.

Pedras, M.S.C., Adio, A.M., Suchy, M., Okinyo, D.P.O., Zheng, Q.A., Jha, M., Sarwar, M.G., 2006. Detection, characterization and identification of crucifer phytoalexins using high performance liquid chromatography with diode array detection and electrospray ionization mass spectrometry. Journal of Chromatography A 1133, 391–411.

Pedras, M.S.C., Ahiahonu, P.W.K., 2005. Metabolism and detoxification of phytoalexins and analogs by phytopathogenic fungi. Phytochemistry 66, 391–411.

Pedras, M.S.C., Zheng, Q.A., Ravi, G.S., 2007a. The first naturally occurring aromatic isothiocyanates, rapalexins A and B, are cruciferous phytoalexins. Chemical Communications, 368–370.

Pedras, M.S.C., Zheng, Q.A., Sarma-Mamillapalle, V.K., 2007b. The phytoalexins from Brassicaceae: structure, biological activity, synthesis and biosynthesis. Natural Product Communications 2, 319–330.

Pidskalny, R.S., Rimmer, S.R., 1985. Virulence of *Albugo candida* from turnip rape (*Brassica campestris*) and mustard (*Brassica juncea*) on various crucifers. Canadian Journal of Plant Pathology 7, 283–286.

Przybylski, R., Mag, T., M Eskin, N.A., McDonald, B.E., 2005. Canola oil, sixth ed.. In: Fereidoon, S. (Ed.), Bailey's Industrial Oil and Fat Products, vol. 2 Springer, Berlin, pp. 61–121.

Rimmer, S.R., Mathur, S., Wu, C.R., 2000. Virulence of isolates of *Albugo candida* from Western Canada to *Brassica* species. Canadian Journal of Plant Pathology 22, 229–235.

Rolland, F., Baena-Gonzalez, E., Sheen, J., 2006. Sugar sensing and signalling in plants: conserved and novel mechanisms. Annual Review of Plant Biology 57, 675–709.

Rouxel, T., Kollmann, A., Boulidard, L., Mithen, R., 1991. Abiotic elicitation of indole phytoalexins and resistance to *Leptosphaeria maculans* within Brassiceae. Planta 184, 271–278.

Tan, J.W., Bednarek, P., Liu, J.K., Schneider, B., Svatos, A., Hahlbrock, K., 2004. Universally occurring phenylpropanoid and species–species indolic metabolites in infected and uninfected *Arabidopsis thaliana* roots and leaves. Phytochemistry 65, 691–699.

Thieme, H., Winkler, H.J., 1969. On the presence of lignan glycosides in the family *Forsythia* 4. Isolation of coniferin. Die Pharmazie 24, 292–293.

Veronese, P., Chen, X., Bluhm, B., Salmeron, J., Dietrich, R., Mengiste, T., 2004. The BOS loci of *Arabidopsis* are required for resistance to *Botrytis cinerea* infection. Plant Journal 40, 558–574.

Voit, O.E., 2003. Biochemical and genomic regulation of the trehalose cycle in yeast: review of observations and canonical model analysis. Journal of Theoretical Biology 223, 55–78.

Von Röpenack, E., Parr, A., Schulze-Lefert, P., 1998. Structural analyses and dynamics of soluble and cell wall-bound phenolics in a broad spectrum resistance to the powdery mildew fungus in barley. Journal of Biological Chemistry 273, 9013–9022.

Whetten, R.W., Sederoff, R., 1995. Lignin biosynthesis. Plant Cell 7, 1001–1013.

Widarto, H.T., Van der Meijden, E., Lefeber, A.W.M., Erkelens, C., Kim, H.K., Choi, Y.H., Verpoorte, R., 2006. Metabolomic differentiation of *Brassica rapa* leaves attacked by herbivore using two dimentional nuclear magnetic resonance spectroscopy. Journal of Chemical Ecology 32, 1428–2417.

Wolbis, M., Krolikowska, M., 1988. Flavonol glycosides from *Sedum acre*. Phytochemistry 27, 3941–3943.